Introduction to Fluorescence Techniques

Fluorescent probes enable researchers to detect particular components of complex biomolecular assemblies, including live cells, with exquisite sensitivity and selectivity. The purpose of this introduction is to briefly outline fluorescence techniques for newcomers to the field.

The Fluorescence Process

Fluorescence is the result of a three-stage process that occurs in certain molecules (generally polyaromatic hydrocarbons or heterocycles) called fluorophores or fluorescent dyes. A fluorescent probe is a fluorophore designed to localize within a specific region of a biological specimen or to respond to a specific stimulus. The process responsible for the fluorescence of fluorescent probes and other fluorophores is illustrated by the simple electronic-state diagram (Jablonski diagram) shown in Figure 1.

Stage 1 : Excitation

A photon of energy $h\upsilon_{EX}$ is supplied by an external source such as an incandescent lamp or a laser and absorbed by the fluorophore, creating an excited electronic singlet state (S_1'). This process distinguishes fluorescence from chemiluminescence, in which the excited state is populated by a chemical reaction.

Stage 2 : Excited-State Lifetime

The excited state exists for a finite time (typically 1–10 nanoseconds). During this time, the fluorophore undergoes conformational changes and is also subject to a multitude of possible interactions with its molecular environment. These processes have two important consequences. First, the energy of S_1' is partially dissipated, yielding a relaxed singlet excited state (S_1) from which fluorescence emission originates. Second, not all the molecules initially excited by absorption (Stage 1) return to the ground state (S_0) by fluorescence emission. Other processes such as collisional quenching, fluorescence resonance energy transfer (FRET, see Section 1.3) and intersystem crossing (see below) may also depopulate S_1. The fluorescence quantum yield, which is the ratio of the number of fluorescence photons emitted (Stage 3) to the number of photons absorbed (Stage 1), is a measure of the relative extent to which these processes occur.

Stage 3 : Fluorescence Emission

A photon of energy $h\upsilon_{EM}$ is emitted, returning the fluorophore to its ground state S_0. Due to energy dissipation during the excited-state lifetime, the energy of this photon is lower, and therefore of longer wavelength, than the excitation photon $h\upsilon_{EX}$. The difference in energy or wavelength represented by ($h\upsilon_{EX} - h\upsilon_{EM}$) is called the Stokes shift. The Stokes shift is fundamental to the sensitivity of fluorescence techniques because it allows emission photons to be detected against a low background, isolated from excitation photons. In contrast, absorption spectrophotometry requires measurement of transmitted light relative to high incident light levels at the same wavelength.

Fluorescence Spectra

The entire fluorescence process is cyclical. Unless the fluorophore is irreversibly destroyed in the excited state (an important phenomenon known as photobleaching, see below), the same fluorophore can be repeatedly excited and detected. The fact that a single fluorophore can generate many thousands of detectable photons is fundamental to the high sensitivity of fluorescence detection techniques. For polyatomic molecules in solution, the discrete electronic transitions represented by $h\upsilon_{EX}$ and $h\upsilon_{EM}$ in Figure 1 are replaced by rather broad energy spectra called the fluorescence excitation spectrum and fluorescence emission spectrum, respectively. The bandwidths of these spectra are parameters of particular importance for applications in which two or more different fluorophores are simultaneously detected (see below). With few exceptions, the fluorescence excitation spectrum of a single fluorophore species in dilute solution is identical to its absorption spectrum. Under the same conditions, the fluorescence emission spectrum is independent of the excitation wavelength, due to the partial dissipation of excitation energy during the excited-state lifetime, as illustrated in Figure 1. The emission intensity is proportional to the amplitude of the fluorescence excitation spectrum at the excitation wavelength (Figure 2).

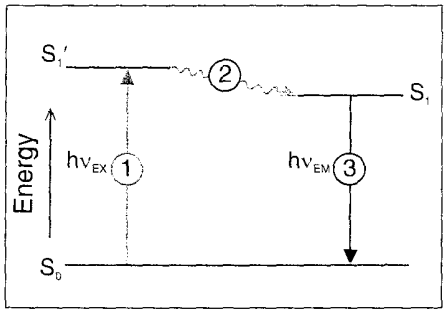

Figure 1 Jablonski diagram illustrating the processes involved in the creation of an excited electronic singlet state by optical absorption and subsequent emission of fluorescence. The labeled stages 1, 2 and 3 are explained in the adjoining text.

Fluorescence Detection

Fluorescence Instrumentation

Four essential elements of fluorescence detection systems can be identified from the preceding discussion: 1) an excitation source, 2) a fluorophore, 3) wavelength filters to isolate emission photons from excitation photons and 4) a detector that registers emission photons and produces a recordable output, usually as an electrical signal or a photographic image. Regardless of the application, compatibility of these four elements is essential for optimizing fluorescence detection.

Fluorescence instruments are primarily of four types, each providing distinctly different information:

- **Spectrofluorometers and microplate readers** measure the *average* properties of bulk (µL to mL) samples.
- **Fluorescence microscopes** resolve fluorescence as a function of spatial coordinates in two or three dimensions for microscopic objects (less than ~0.1 mm diameter).
- **Fluorescence scanners**, including microarray readers, resolve fluorescence as a function of spatial coordinates in two dimensions for macroscopic objects such as electrophoresis g blots and chromatograms.
- **Flow cytometers** measure fluorescence per cell in a flo stream, allowing subpopulations within a large sample identified and quantitated.

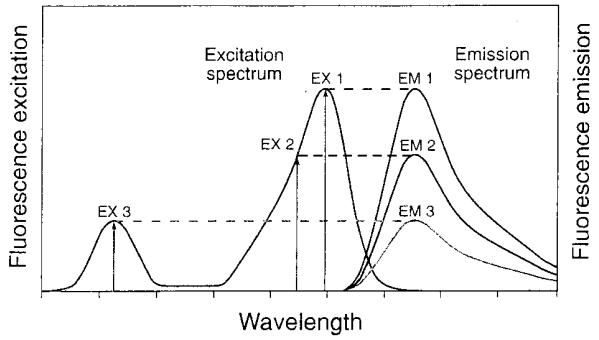

Figure 2 Excitation of a fluorophore at three different wavelengths (EX 1, EX 2, EX 3) does not change the emission profile but does produce variations in fluorescence emission intensity (EM 1, EM 2, EM 3) that correspond to the amplitude of the excitation spectrum.

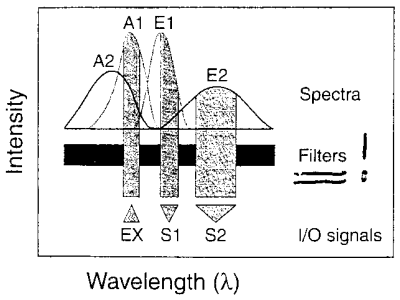

Figure 3 Fluorescence detection of mixed species. Excitation (EX) in overlapping absorption bands A1 and A2 produces two fluorescent species with spectra E1 and E2. Optical filters isolate quantitative emission signals S1 and S2.

Other types of instrumentation that use fluorescence de include capillary electrophoresis apparatus, DNA sequenc microfluidic devices. Each type of instrument produces dif measurement artifacts and makes different demands on the rescent probe. For example, although photobleaching is oft significant problem in fluorescence microscopy, it is not a impediment in flow cytometry or DNA sequencers becaus dwell time of individual cells or DNA molecules in the exc beam is short.

Fluorescence Signals

Fluorescence intensity is quantitatively dependent on th parameters as absorbance — defined by the Beer–Lambert the product of the molar extinction coefficient, optical path and solute concentration — as well as on the fluorescence tum yield of the dye and the excitation source intensity anc rescence collection efficiency of the instrument. In dilute sc or suspensions, fluorescence intensity is linearly proportio these parameters. When sample absorbance exceeds about a 1 cm pathlength, the relationship becomes nonlinear and surements may be distorted by artifacts such as self-absorp and the inner-filter effect.[1] Because fluorescence quantitati dependent on the instrument, fluorescent reference standar essential for calibrating measurements made at different ti using different instrument configurations.[2–4] To meet these quirements, Molecular Probes offers high-precision fluores microsphere reference standards for fluorescence microsco flow cytometry and a set of ready-made fluorescent standa solutions for spectrofluorometry (Section 24.1, Section 24.

A spectrofluorometer is extremely flexible, providing c ous ranges of excitation and emission wavelengths. Laser-s ning microscopes and flow cytometers, however, require p that are excitable at a single fixed wavelength. In contemp instruments, the excitation source is usually the 488 nm sp line of the argon-ion laser. As shown in Figure 3, separatio the fluorescence emission signal (S1) from Rayleigh-scatte excitation light (EX) is facilitated by a large fluorescence S shift (i.e., separation of A1 and E1). Biological samples lat with fluorescent probes typically contain more than one flu cent species, making signal-isolation issues more complex. tional optical signals, represented in Figure 3 as S2, may b to background fluorescence or to a second fluorescent prob

Background Fluorescence

Fluorescence detection sensitivity is severely compromi background signals, which may originate from endogenous ple constituents (referred to as autofluorescence) or from u bound or nonspecifically bound probes (referred to as reag background). Detection of autofluorescence can be minimi either by selecting filters that reduce the transmission of E tive to E1 or by selecting probes that absorb and emit at lo wavelengths. Although narrowing the fluorescence detecti bandwidth increases the resolution of E1 and E2, it also co

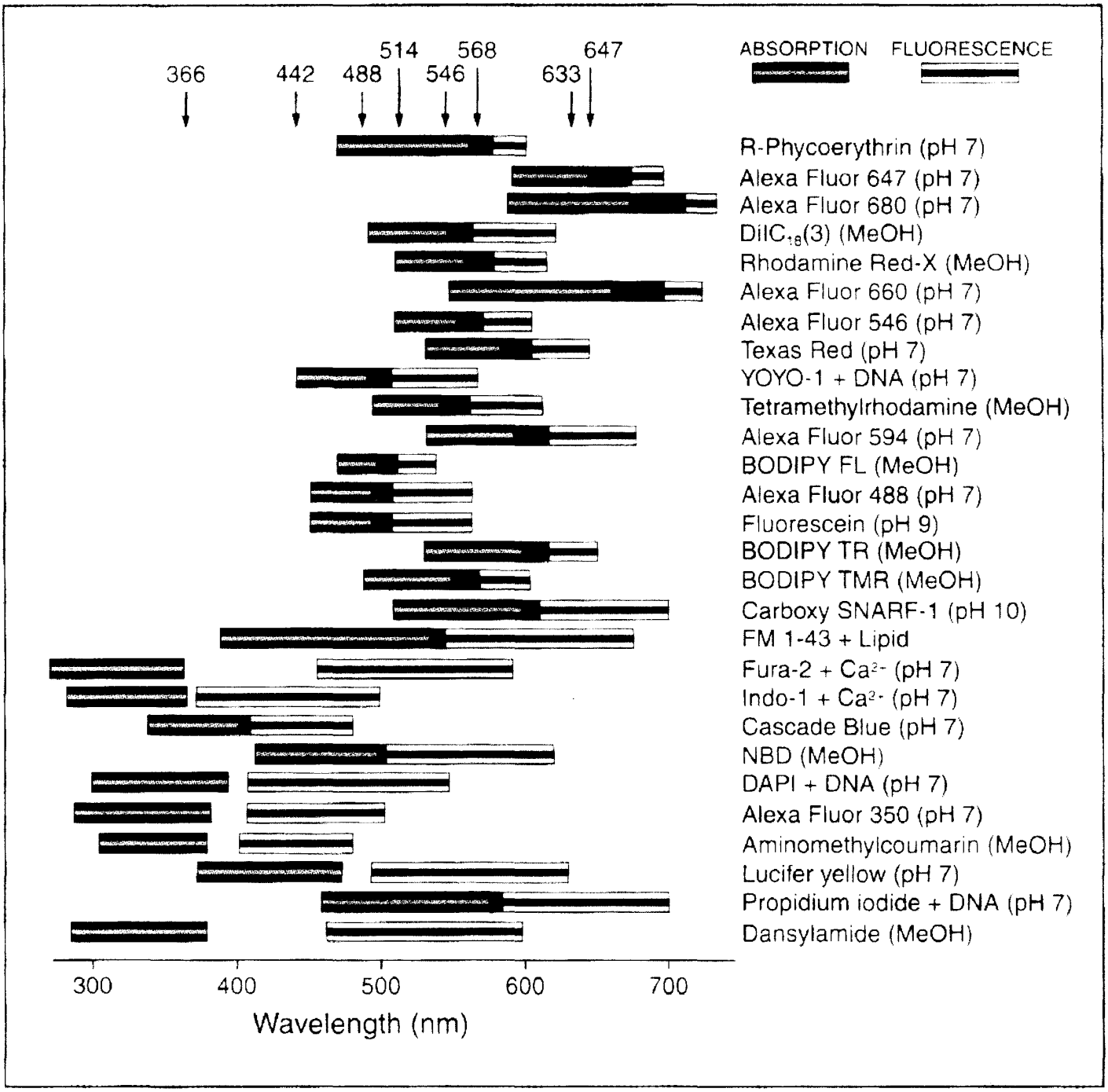

Figure 4 Absorption and fluorescence spectral ranges for 28 fluorophores of current practical importance. The range encompasses only those values of the absorbance or the fluorescence emission that are >25% of the maximum value. Fluorophores are arranged vertically in rank order of the maximum molar extinction coefficient (ε_{max}), in either methanol or aqueous buffer as specified. Some important excitation source lines are indicated on the upper horizontal axis.

mises the overall fluorescence intensity detected. Signal distortion caused by autofluorescence of cells, tissues and biological fluids is most readily minimized by using probes that can be excited at >500 nm. Furthermore, at longer wavelengths, light scattering by dense media such as tissues is much reduced, resulting in greater penetration of the excitation light.[5]

Multicolor Labeling Experiments

A multicolor labeling experiment entails the deliberate introduction of two or more probes to simultaneously monitor different biochemical functions. This technique has major applications in flow cytometry,[6,7] DNA sequencing,[8,9] fluorescence *in situ* hybridization [10,11] and fluorescence microscopy.[12,13] Signal isolation and data analysis are facilitated by maximizing the spectral separation of the multiple emissions (E1 and E2 in Figure 3). Consequently, fluorophores with narrow spectral bandwidths, such as Molecular Probes' Alexa Fluor dyes (Section 1.3) and BODIPY dyes (Section 1.4), are particularly useful in multicolor applications.[8] An ideal combination of dyes for multicolor labeling would exhibit strong absorption at a coincident excitation wavelength and well-separated emission spectra (Figure 3). Unfortunately, it is not easy to find single dyes with the requisite combination of a large extinction coefficient for absorption and a large Stokes shift [14] (see Limitations of Low Molecular Weight Dyes in Section 6.5).

Ratiometric Measurements

In some cases, for example the Ca^{2+} indicators fura-2 and indo-1 (Section 20.2) and the pH indicators BCECF, SNARF and SNAFL (Section 21.2), the free and ion-bound forms of fluorescent ion indicators have different emission or excitation spectra. With this type of indicator, the ratio of the optical signals (S1 and S2 in Figure 3) can be used to monitor the association equilibrium and to calculate ion concentrations. Ratiometric measurements eliminate distortions of data caused by photobleaching and variations in probe loading and retention, as well as by instrumental factors such as illumination stability.[15] For a thorough discussion of ratiometric techniques, see Loading and Calibration of Intracellular Ion Indicators (Section 20.1).

Fluorescence Output of Fluorophores

Comparing Different Dyes

Fluorophores currently used as fluorescent probes offer sufficient permutations of wavelength range, Stokes shift and spectral bandwidth to meet requirements imposed by instrumentation (e.g., 488 nm excitation), while allowing flexibility in the design of multicolor labeling experiments (Figure 4). The fluorescence output of a given dye depends on the efficiency with which it absorbs and emits photons, and its ability to undergo repeated excitation/emission cycles. Absorption and emission efficiencies are most usefully quantified in terms of the molar extinction coefficient (ε) for absorption and the quantum yield (QY) for fluorescence. Both are constants under specific environmental conditions. The value of ε is specified at a single wavelength (usually the absorption maximum), whereas QY is a measure of the total photon emission over the entire fluorescence spectral profile. Fluorescence intensity per dye molecule is proportional to the product of ε and QY. The range of these parameters among fluorophores of current practical importance is approximately 5000 to 200,000 $cm^{-1}M^{-1}$ for ε and 0.05 to 1.0 for QY. Phycobiliproteins such as R-phycoerythrin (Section 6.4) have multiple fluorophores on each protein and consequently have much larger extinction coefficients (on the order of 2×10^6 $cm^{-1}M^{-1}$) than low molecular weight fluorophores.

Photobleaching

Under high-intensity illumination conditions, the irreversible destruction or photobleaching of the excited fluorophore becomes the factor limiting fluorescence detectability. The multiple photochemical reaction pathways responsible for photobleaching of fluorescein have been investigated and described in considerable detail.[16,17] Some pathways include reactions between adjacent dye molecules, making the process considerably more complex in labeled biological specimens than in dilute solutions of free dye. In all cases, photobleaching originates from the triplet excited state, which is created from the singlet state (S_1, Figure 1) via an excited-state process called intersystem crossing.

The most effective remedy for photobleaching is to maximize detection sensitivity, which allows the excitation intensity to be reduced. Detection sensitivity is enhanced by low-light detection devices such as CCD cameras, as well as by high–numerical aperture objectives and the widest emission bandpass filters compatible with satisfactory signal isolation. Alternatively, a less photolabile fluorophore may be substituted in the experiment. Molecular Probes' Alexa Fluor 488 dye is an important fluorescein substitute that provides significantly greater photostability than fluorescein (Figure 1.9, Figure 1.42), yet is compatible with standard fluorescein optical filters. Antifade reagents such as

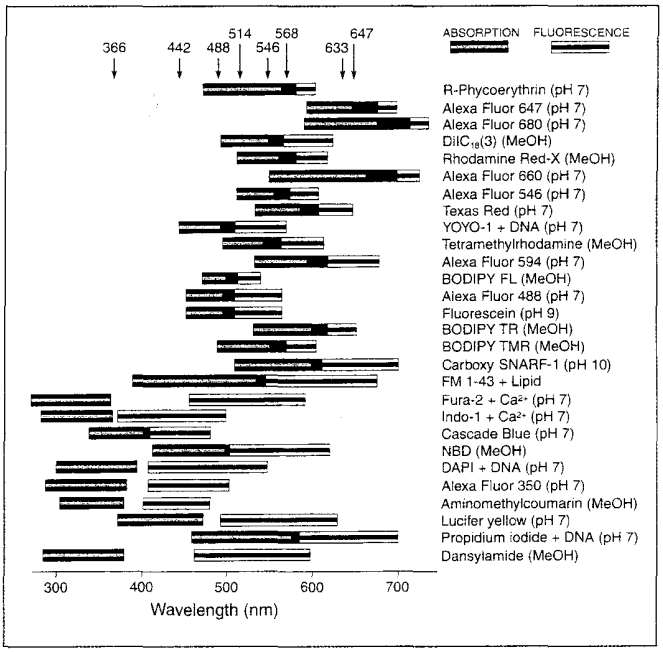

Figure 4 Absorption and fluorescence spectral ranges for 28 fluorophores of current practical importance. The range encompasses only those values of the absorbance or the fluorescence emission that are >25% of the maximum value. Fluorophores are arranged vertically in rank order of the maximum molar extinction coefficient (ε_{max}), in either methanol or aqueous buffer as specified. Some important excitation source lines are indicated on the upper horizontal axis.

Molecular Probes' *SlowFade* and ProLong products (Section 24.1) can also be applied to reduce photobleaching; however, they are usually incompatible with live cells. In general, it is difficult to predict the necessity for and effectiveness of such countermeasures because photobleaching rates are dependent to some extent on the fluorophore's environment.[17–19]

Signal Amplification

The most straightforward way to enhance fluorescence signals is to increase the number of fluorophores available for detection. Fluorescent signals can be amplified using 1) avidin–biotin or antibody–hapten secondary detection techniques, 2) enzyme-labeled secondary detection reagents in conjunction with fluorogenic substrates[20,21] or 3) probes that contain multiple fluorophores such as phycobiliproteins and Molecular Probes' FluoSpheres fluorescent microspheres. Our most sensitive reagents and methods for signal amplification are discussed in Chapter 6.

Simply increasing the probe concentration can be counterproductive and often produces marked changes in the probe's chemical and optical characteristics. It is important to note that the effective intracellular concentration of probes loaded by bulk permeabilization methods (see Loading and Calibration of Intracellular Ion Indicators in Section 20.1) is usually much higher (>tenfold) than the extracellular incubation concentration. Also, increased labeling of proteins or membranes ultimately leads to precipitation of the protein or gross changes in membrane permeability. Antibodies labeled with more than four to six fluorophores per protein may exhibit reduced specificity and reduced binding affinity. Furthermore, at high degrees of substitution, the extra fluorescence obtained per added fluorophore typically decreases due to self-quenching (Figure 1.49).

Environmental Sensitivity of Fluorescence

Fluorescence spectra and quantum yields are generally more dependent on the environment than absorption spectra and extinction coefficients. For example, coupling a single fluorescein label to a protein typically reduces fluorescein's QY ~60% but only decreases its ε by ~10%. Interactions either between two adjacent fluorophores or between a fluorophore and other species in the surrounding environment can produce environment-sensitive fluorescence.

Fluorophore–Fluorophore Interactions

Fluorescence quenching can be defined as a bimolecular process that reduces the fluorescence quantum yield without changing the fluorescence emission spectrum; it can result from transient excited-state interactions (collisional quenching) or from formation of nonfluorescent ground-state species. Self-quenching is the quenching of one fluorophore by another; it therefore tends to occur when high loading concentrations or labeling densities are used (Figure 1.49, Figure 1.71). Molecular Probes' DQ substrates (Section 10.4) are heavily labeled and therefore highly quenched biopolymers that exhibit dramatic fluorescence enhancement upon enzymatic cleavage[22] (Figure 10.47). Studies of the self-quenching of carboxyfluorescein show that the mechanism involves energy transfer to nonfluorescent dimers.[23]

Fluorescence resonance energy transfer (FRET, see Section 1.3) is a strongly distance-dependent excited-state interaction in which emission of one fluorophore is coupled to the excitation of another.

Some excited fluorophores interact to form excimers, which are excited-state dimers that exhibit altered emission spectra. Excimer formation by the polyaromatic hydrocarbon pyrene is described in Section 13.2 (see especially Figure 13.8).

Because they all depend on the interaction of adjacent fluorophores, self-quenching, FRET and excimer formation can be exploited for monitoring a wide array of molecular assembly or fragmentation processes such as membrane fusion (see Assays of Volume Change, Membrane Fusion and Membrane Permeability in Section 14.3), nucleic acid hybridization (Section 8.5), ligand–receptor binding and polypeptide hydrolysis.

Other Environmental Factors

Many other environmental factors exert influences on fluorescence properties. The three most common are:

- Solvent polarity (solvent in this context includes interior regions of cells, proteins, membranes and other biomolecular structures)
- Proximity and concentrations of quenching species
- pH of the aqueous medium
- Temperature

Fluorescence spectra may be strongly dependent on solvent. This characteristic is most often observed with fluorophores that have large excited-state dipole moments, resulting in fluorescence spectral shifts to longer wavelengths in polar solvents. Representative fluorophores include the aminonaphthalenes such as prodan, badan (Figure 2.23) and dansyl, which are effective probes of environmental polarity in, for example, a protein's interior.[24]

Binding of a probe to its target can dramatically affect its fluorescence quantum yield (see Monitoring Protein-Folding Processes with Anilinonaphthalenesulfonate Dyes in Section 13.5). Probes that have a high fluorescence quantum yield when bound to a particular target but are otherwise effectively nonfluorescent yield extremely low reagent background signals (see above). Molecular Probes' ultrasensitive SYBR Green, SYBR Gold, SYTO, PicoGreen, RiboGreen and OliGreen nucleic acid stains (Section 8.3, Section 8.4) are prime examples of this strategy. Similarly, fluorogenic enzyme substrates, which are nonfluorescent or have only short-wavelength emission until they are converted to fluorescent products by enzymatic cleavage (see below), allow sensitive detection of enzymatic activity.

Extrinsic quenchers, the most ubiquitous of which are paramagnetic species such as O_2 and heavy atoms such as iodide, reduce fluorescence quantum yields in a concentration-dependent manner. If quenching is caused by collisional interactions, as is usually the case, information on the proximity of the fluorophore and quencher and their mutual diffusion rate can be derived. This quenching effect has been used productively to measure chloride-ion flux in cells (Section 22.2). Many fluorophores are also quenched by proteins. Examples are NBD, fluorescein and BODIPY dyes, in which the effect is apparently due to charge-transfer interactions with aromatic amino acid residues.[25–27] Consequently, antibodies raised against these fluorophores are effective and highly specific fluorescence quenchers (Section 7.4).

Fluorophores such as BCECF and carboxy SNARF-1 that have strongly pH-dependent absorption and fluorescence characteristics can be used as physiological pH indicators. Fluorescein and hydroxycoumarins (umbelliferones) are further examples of this type of fluorophore. Structurally, pH sensitivity is due to a reconfiguration of the fluorophore's π-electron system that occurs upon protonation. Molecular Probes' BODIPY FL fluorophore and the Alexa Fluor 488 dye, both of which lack protolytically ionizable substituents, provide spectrally equivalent alternatives to fluorescein for applications requiring a pH-*in*sensitive probe (Section 1.3, Section 1.4).

Modifying Environmental Sensitivity of a Fluorophore

The environmental sensitivity of a fluorophore can be transformed by structural modifications to achieve a desired probe specificity. For example, conversion of the prototropic 3′- and 6′-hydroxyl groups of fluorescein to acetate esters yields colorless and nonfluorescent fluorescein diacetate. This derivatization causes fluorescein to adopt the nonfluorescent lactone configuration that is also prevalent at low pH [28] (Figure 21.1); cleavage of the acetates by esterases under appropriate pH conditions releases anionic fluorescein, which is strongly colored and highly fluorescent. Fluorogenic substrates for other hydrolytic enzymes can be created by replacing acetates with other appropriate functional groups such as sugar ethers (glycosides, Section 10.2) or phosphate esters (Section 10.3). Furthermore, unlike fluorescein, fluorescein diacetate is uncharged and therefore somewhat membrane permeant. This property forms the basis of an important noninvasive method for loading polar fluorescent indicators into cells in the form of membrane-permeant precursors that can be activated by intracellular esterases [29] (see Loading and Calibration of Intracellular Ion Indicators in Section 20.1).

References

1. Analyst 119, 417 (1994); **2.** Methods Cell Biol 42 Pt B, 605 (1994); **3.** Methods Cell Biol 30, 113 (1989); **4.** Luminescence Applications in Biol, Chem, Environ and Hydrol Sciences, Goldberg MC, Ed. pp. 98–126 (1989); **5.** J Microsc 176, 281 (1994); **6.** Methods Cell Biol 41, 61 (1994); **7.** Methods 2, 192 (1991); **8.** Science 271, 1420 (1996); **9.** Anal Biochem 223, 39 (1994); **10.** Proc Natl Acad Sci U S A 89, 1388 (1992); **11.** Cytometry 11, 126 (1990); **12.** Methods Cell Biol 38, 97 (1993); **13.** Methods Cell Biol 30, 449 (1989); **14.** Optical Microscopy for Biology, Herman B, Jacobson K, Eds. pp. 143–157 (1990); **15.** Methods Cell Biol 56, 237 (1998); **16.** Biophys J 70, 2959 (1996); **17.** Biophys J 68, 2588 (1995); **18.** J Cell Biol 100, 1309 (1985); **19.** J Org Chem 38, 1057 (1973); **20.** Cytometry 23, 48 (1996); **21.** J Histochem Cytochem 43, 77 (1995); **22.** Anal Biochem 251, 144 (1997); **23.** Anal Biochem 172, 61 (1988); **24.** Nature 319, 70 (1986); **25.** Biophys J 69, 716 (1995); **26.** Biochemistry 16, 5150 (1977); **27.** Immunochemistry 14, 533 (1977); **28.** Spectrochim Acta A 51, 7 (1995); **29.** Proc Natl Acad Sci U S A 55, 134 (1966).

Selected Books and Articles

The preceding discussion has introduced some general principles to consider when selecting a fluorescent probe. Application-specific details are addressed in subsequent chapters of this *Handbook*. For in-depth treatments of fluorescence techniques and their biological applications, the reader is referred to the many excellent books and review articles listed below.

Principles of Fluorescence Detection

Brand, L. and Johnson, M.L., Eds., *Fluorescence Spectroscopy (Methods in Enzymology, Volume 278)*, Academic Press (1997).

Cantor, C.R. and Schimmel, P.R., *Biophysical Chemistry Part 2*, W.H. Freeman (1980) pp. 433–465.

Dewey, T.G., Ed., *Biophysical and Biochemical Aspects of Fluorescence Spectroscopy*, Plenum Publishing (1991).

Guilbault, G.G., Ed., *Practical Fluorescence, Second Edition*, Marcel Dekker (1990).

Lakowicz, J.R., Ed., *Topics in Fluorescence Spectroscopy: Techniques (Volume 1, 1991); Principles (Volume 2, 1991); Biochemical Applications (Volume 3, 1992); Probe Design and Chemical Sensing (Volume 4, 1994); Nonlinear and Two-Photon Induced Fluorescence (Volume 5, 1997); Protein Fluorescence (Volume 6, 2000)*, Plenum Publishing.

Lakowicz, J.R., *Principles of Fluorescence Spectroscopy, Second Edition*, Plenum Publishing (1999).

Mathies, R.A., Peck, K. and Stryer, L., "Optimization of High-Sensitivity Fluorescence Detection," Anal Chem 62, 1786–1791 (1990).

Oldham, P.B., McCarroll, M.E., McGown, L.B. and Warner, I.M., "Molecular Fluorescence, Phosphorescence, and Chemiluminescence Spectrometry," Anal Chem 72, 197R–209R (2000).

Royer, C.A., "Approaches to Teaching Fluorescence Spectroscopy," Biophys J 68, 1191–1195 (1995).

Sharma, A. and Schulman, S.G., *Introduction to Fluorescence Spectroscopy*, John Wiley and Sons (1999).

Valeur, B., *Molecular Fluorescence: Principles and Applications*, John Wiley and Sons (2002).

Fluorophores and Fluorescent Probes

Berlman, I.B., *Handbook of Fluorescence Spectra of Aromatic Molecules, Second Edition*, Academic Press (1971).

Czarnik, A.W., Ed., *Fluorescent Chemosensors for Ion and Molecule Recognition (ACS Symposium Series 538)*, American Chemical Society (1993).

Drexhage, K.H., "Structure and Properties of Laser Dyes" in *Dye Lasers, Third Edition*, F.P. Schäfer, Ed., Springer-Verlag, (1990) pp. 155–200.

Giuliano, K.A. *et al.*, "Fluorescent Protein Biosensors: Measurement of Molecular Dynamics in Living Cells," Ann Rev Biophys Biomol Struct 24, 405–434 (1995).

Green, F.J., *The Sigma-Aldrich Handbook of Stains, Dyes and Indicators*, Aldrich Chemical Company (1990).

Griffiths, J., *Colour and Constitution of Organic Molecules*, Academic Press (1976).

Haugland, R.P., "Antibody Conjugates for Cell Biology" in *Current Protocols in Cell Biology*, J.S. Bonifacino, M. Dasso, J. Lippincott-Schwartz, J.B. Harford and K.M. Yamada, Eds., John Wiley and Sons (2000) pp. 16.5.1–16.5.22.

Haugland, R.P., "Spectra of Fluorescent Dyes Used in Flow Cytometry," Meth Cell Biol 42, 641–663 (1994).

Hermanson, G.T., *Bioconjugate Techniques*, Academic Press (1996). **Available from Molecular Probes** (B-7884, Section 24.6).

Johnson, I.D., Ryan, D. and Haugland, R.P., "Comparing Fluorescent Organic Dyes for Biomolecular Labeling" in *Methods in Nonradioactive Detection*, G.C. Howard, Ed., Appleton and Lange (1993) pp. 47–68.

Johnson, I.D., "Fluorescent Probes for Living Cells," Histochem J 30, 123–140 (1998).

Kasten, F.H., "Introduction to Fluorescent Probes: Properties, History and Applications" in *Fluorescent and Luminescent Probes for Biological Activity*, W.T. Mason, Ed., Academic Press (1993) pp. 12–33.

Krasovitskii, B.M. and Bolotin, B.M., *Organic Luminescent Materials*, VCH Publishers (1988).

Lakowicz, J.R., Ed., *Topics in Fluorescence Spectroscopy: Probe Design and Chemical Sensing (Volume 4)*, Plenum Publishing (1994).

Mason, W.T., Ed., *Fluorescent and Luminescent Probes for Biological Activity*, Second Edition, Academic Press (1999). **Available from Molecular Probes** (F-14944, Section 24.6).

Marriott, G., Ed., *Caged Compounds (Methods in Enzymology, Volume 291)*, Academic Press (1998).

Tsien, R.Y., "The Green Fluorescent Protein," Ann Rev Biochem 67, 509–544 (1998).

Waggoner, A.S., "Fluorescent Probes for Cytometry" in *Flow Cytometry and Sorting, Second Edition*, M.R. Melamed, T. Lindmo and M.L. Mendelsohn, Eds., Wiley-Liss (1990) pp. 209–225.

Wells, S. and Johnson, I., "Fluorescent Labels for Confocal Microscopy" in *Three-Dimensional Confocal Microscopy: Volume Investigation of Biological Systems*, J.K. Stevens, L.R. Mills and J.E. Trogadis, Eds., Academic Press (1994) pp. 101–129.

Fluorescence Microscopy

Allan, V., Ed., *Protein Localization by Fluorescence Microscopy: A Practical Approach*, Oxford University Press (1999).

Andreeff, M. and Pinkel, D., Eds., *Introduction to Fluorescence In Situ Hybridization: Principles and Clinical Applications*, John Wiley and Sons (1999).

Conn, P.M., Ed., *Confocal Microscopy (Methods in Enzymology, Volume 307)*, Academic Press (1999).

Denk, W. and Svoboda, K., "Photon Upmanship: Why Multiphoton Imaging is more than a Gimmick," Neuron 18, 351–357 (1997).

Diaspro, A., Ed., *Confocal and Two-Photon Microscopy: Foundations, Applications and Advances*, John Wiley and Sons (2001).

Herman, B., *Fluorescence Microscopy, Second Edition*, BIOS Scientific Publishers (1998). **Available from Molecular Probes** (F-14942, Section 24.6)

Inoué, S. and Spring, K.R., *Video Microscopy, Second Edition*, Plenum Publishing (1997).

Matsumoto, B., Ed., *Cell Biological Applications of Confocal Microscopy (Methods in Cell Biology, Volume 38)*, Academic Press (1993).

Murphy, D.B., *Fundamentals of Light Microscopy and Electronic Imaging*, John Wiley and Sons (2001). **Available from Molecular Probes** (F-24840, Section 24.6).

Pawley, J.B., Ed., *Handbook of Biological Confocal Microscopy, Second Edition*, Plenum Publishing (1995).

Paddock, S., Ed., *Confocal Microscopy (Methods in Molecular Biology, Volume 122)*, Humana Press (1998). **Available from Molecular Probes** (C-14946, Section 24.6).

Periasamy, A., Ed., *Methods in Cellular Imaging*, Oxford University Press (2001).

Rizzuto, R., and Fasolato, C., Eds., *Imaging Living Cells*, Springer-Verlag (1999).

Sheppard, C.J.R. and Shotton, D.M., *Confocal Laser Scanning Microscopy*, BIOS Scientific Publishers (1997).

Slavík, J., *Fluorescence Microscopy and Fluorescent Probes*, Plenum Publishing (1996).

Stevens, J.K., Mills, L.R. and Trogadis, J.E., Eds., *Three-Dimensional Confocal Microscopy: Volume Investigation of Biological Systems*, Academic Press (1994).

Taylor, D.L. and Wang, Y.L., Eds., *Fluorescence Microscopy of Living Cells in Culture, Parts A and B (Methods in Cell Biology, Volumes 29 and 30)*, Academic Press (1989).

Wang, X.F. and Herman, B., Eds., *Fluorescence Imag Microscopy*, John Wiley and Sons (1996).

Yuste, R., Lanni, F. and Konnerth, A., *Imaging Neuro Manual*, Cold Spring Harbor Laboratory Press (2000) **Molecular Probes** (I-24830, Section 24.6).

Flow Cytometry

Darzynkiewicz, Z., Crissman, H.A. and Robinson, J.F *Edition Parts A and B (Methods in Cell Biology, Volu* demic Press (2001).

Davey, H.M. and Kell, D.B., "Flow Cytometry and C neous Microbial Populations: The Importance of Sing Microbiological Rev 60, 641–696 (1996).

Gilman-Sachs, A., "Flow Cytometry," Anal Chem 66,

Givan, A.L., *Flow Cytometry: First Principles, Secon* and Sons (2001).

Jaroszeski, M.J. and Heller, R., Eds., *Flow Cytometry Molecular Biology, Volume 91)*, Humana Press (1997

Lloyd, D., Ed., *Flow Cytometry in Microbiology*, Spri

Melamed, M.R., Lindmo, T. and Mendelsohn, M.L., F *and Sorting, Second Edition*, Wiley-Liss (1990).

Ormerod, M.G., Ed., *Flow Cytometry: A Practical Ap* Oxford University Press (2000).

Robinson, J.P., Ed., *Current Protocols in Cytometry*, J (1997).

Shapiro, H.M., "Optical Measurement in Cytometry: tion, Absorption and Fluorescence," Meth Cell Biol 6.

Shapiro, H.M., *Practical Flow Cytometry, Third Editi*

Watson, J.V., Ed., *Introduction to Flow Cytometry*, Ca Press (1991).

Weaver, J.L., "Introduction to Flow Cytometry," Meth (2000). This journal issue also contains 10 review arti cytometry applications.

Other Fluorescence Measurement Techniqu

Goldberg, M.C., Ed., *Luminescence Applications in B Environmental and Hydrological Sciences (ACS Symp* American Chemical Society (1989).

Gore, M., Ed., *Spectrophotometry and Spectrofluorim proach, Second Edition*, Oxford University Press (200

Hemmilä, I.A., *Applications of Fluorescence in Immu* and Sons (1991).

Patton, W.F., "A Thousand Points of Light: The Appli Detection Technologies to Two-dimensional Gel Elect mics," Electrophoresis 21, 1123–1144 (2000).

Rampal, J.B., Ed., *DNA Arrays: Methods and Protoco lar Biology, Volume 170)*, Humana Press (2001). **Avail Probes** (D-24835, Section 24.6).

Schena, M., Ed., *DNA Microarrays: A Practical Appr* Press (1999).

Schena, M., Ed., *Microarray Biochip Technology*, Bio (2000).

Books that are available from Molecular P described in Section 24.6.

78 Heterologous Expression of the Green Fluorescent Protein

INTRODUCTION

The green fluorescent protein GFP is a 238-amino-acid protein originally cloned from the jellyfish *Aequorea victoria* found in the waters of Friday Harbor, Washington. Similar proteins are expressed in many jellyfish and appear to be responsible for the green light that they emit. In some cnidarians, it is thought that a luciferase produces the energy, via the oxidation of luciferin, to stimulate GFP. However, in *Aequorea*, the protein aequorin stimulates GFP (for review, see Chalfie 1995; Prasher 1995). Most of what we know to date about GFP is based on the clone (GFP 10.1)—or derivatives thereof—originally isolated by Prasher et al. (1992). However, the *Aequorea* genome harbors several similar sequences and more remains to be learned about the properties of these other gene products (Prasher et al. 1992).

The critical observation that revealed the potential utility of GFP as a reporter was made by Chalfie et al. (1994). These authors found that the expression of the cDNA encoding GFP was sufficient to produce the characteristic fluorescence of GFP in either *E. coli* or *C. elegans*. This provided strong evidence that the protein by itself, with no special cofactors or additional proteins, could be a functional fluorophore. Since the publication of that work, many laboratories have exploited this protein in a wide variety of systems. GFP is a unique reporter, since no other agents, such as antibodies, cofactors, or enzyme substrates, are necessary. Moreover, the protein does not appear to affect the cells that contain it, making it possible to identify, follow, and sort living cells that express GFP.

The physical properties of GFP have been well-characterized. The fluorophore in GFP is formed by the cyclization of residues Ser-65, Tyr-66, and Gly-67. GFP undergoes an autocatalytic, oxidative reaction that creates the fluorophore (Heim et al. 1994; Inouye and Tsuji 1994a). This posttranslational formation of the fluorophore occurs with a time constant of nearly 4 hours (Heim et al. 1994). Mutations in the protein have been discovered that increase the speed by which this process occurs—to date, the quickest is S65T (20 minutes) (Heim et al. 1995)—but the rate remains relatively slow and this may constrain its use as a reporter of events that occur rapidly. GFP is pH-sensitive to some extent (Terry et al. 1995), and there are reports that the maturation of the protein is temperature-sensitive (Lim et al. 1995) and can be blocked by reducing agents (Inouye and Tsuji 1994b).

GFP has now been crystallized and its structure has been solved (Ormö et al. 1996; Yang et al. 1996). The structure of GFP can be found at Brookhaven National Laboratory: http://www.pdb.bnl.gov/browse __ it.html. The structure of wild-type GFP (Yang et al. 1996) is I.D. code 1 gfl, and the structure of the S65T mutant (Ormö et al. 1996) is I.D. code 1 ema. The protein consists of an 11-stranded β-barrel that encapsulates a central helix. Little can be omitted from the protein without damaging its structure. This is consistent with a deletion analysis which found that residues 2 through 232 are necessary for the protein's fluorescence (Dopf and Horiagon 1996). Many mutations affect the excitation/emission characteristics of GFP (Cormack et al. 1996; Crameri et al. 1996; Delagrave et al. 1995; Heim et al. 1994, 1995). These mu-

tations are widely distributed across the primary sequence and most are interpretable in the context of the structure of the protein. The mutations fall into two categories: those that affect the chromophore region, which resides in residues 56–72, and those that affect one of the β sheets that interact with the chromophore. The many mutant forms of GFP now available make it possible to select a fluorescent species best suited for a particular experiment or optical detection system.

GFP as a Reporter

The observation that functional GFP can be expressed in *E. coli* led to a variety of attempts to express the protein in many different genera. It soon became apparent that GFP could be successfully used in yeast (Flach et al. 1994; Nabeshima et al. 1995), *Dictyostelium discoideum*, (Maniak et al. 1995), plants (Baulcombe et al. 1995), *C. elegans* (Chalfie et al. 1994; Treinin and Chalfie 1995; Troemel et al. 1995), *Drosophila* (Wang and Hazelrigg 1994; Barthmaier and Fyrberg 1995), amphibians (Tannahill et al. 1995; Wu et al. 1995), mammalian cell lines (Marshall et al. 1995; Misteli et al. 1997), and neurons within the rat brain (Lo et al. 1994).

Furthermore, there are accumulating reports of expression of GFP in animals, for example, in the skin of a mouse, the olfactory neurons of a transgenic mouse, the astrocytes of transgenic mice (A. Messing, pers. comm.), and the noradrenergic neurons in the mouse (T. Hughes et al., pers. comm.). There are several reports that GFP can be used as a reporter in transgenic mice (Chiocchetti et al. 1997; Okabe et al. 1997; Zhuo et al. 1997) and one of these has found evidence that GFP signal can be more sensitive than reporters typically used for transgene analysis (Chiocchetti et al. 1997).

This widespread success indicated that the many potential difficulties in the heterologous expression of a jellyfish protein were not insurmountable obstacles. Despite these early successes, a number of failures revealed features in the original clone that reduced or abolished expression. Sequence in the 5′-untranslated region of the original clone appeared to inhibit expression (see notes in Chalfie et al. 1994); those that have reported successful expression of GFP have employed only the coding region. The Kozak consensus at the start of translation was not optimal, and the codon usage was poorly suited for expression in mammalian cells. By modifying these features, Zolotkin et al. (1996) were able to achieve a significant increase in expression levels in mammalian cells. Similar efforts may be worthwhile in optimizing GFP expression in other genera. Finally, there are cryptic splice sites in the sequence that can, at least in plants, inhibit successful expression (Haseloff and Amos 1995; Reichel et al. 1996; Haseloff et al. 1997).

GFP can be used to identify, without compromising, cells that harbor newly introduced genes. This makes it possible to evaluate rapidly the success of an expression experiment, to identify particular cells that express significant amounts of a particular gene product for biophysical characterization (Marshall et al. 1995), or to screen transgenic animals (Amsterdam et al. 1995; Ikawa et al. 1995; Troemel et al. 1995). The signal produced by GFP is sufficient to sort populations of cells with a fluorescence-activated cell sorter, making it possible to rapidly quantify or select the expressing cells (Cormack et al. 1996; Levy et al. 1996; Valdivia et al. 1996; Zolotkin et al. 1996). These characteristics make this an ideal reporter for expression cloning strategies or the analysis of promoter/enhancer regions (Valdivia et al. 1996).

GFP in Fusion Constructs

Fusion constructs that join GFP to another coding region can provide important insights into the localization of a protein of interest. This is largely because GFP itself is not localized within a cell. In most cell types, the fluorescence of GFP appears to homogeneously fill the cytoplasm, nucleus, and distal processes such as neurites (Chalfie et al. 1994; Marshall et al. 1995). Confocal microscopy reveals that only a small vesicular compartment excludes labeling (see Fig. 78.1). However, this even distribution of GFP does not occur in all cell lines. There are exceptions that make it important to characterize the localization of GFP in a new cell line before trying to interpret the signal a fusion construct produces. For example, in COS cells, GFP produces what appears to be a concentration of signal in the nucleus (Moriyoshi et al. 1996).

The simplest fusion experiments are those that add short sequences to GFP to target the protein to particular compartments such as the plasma membrane

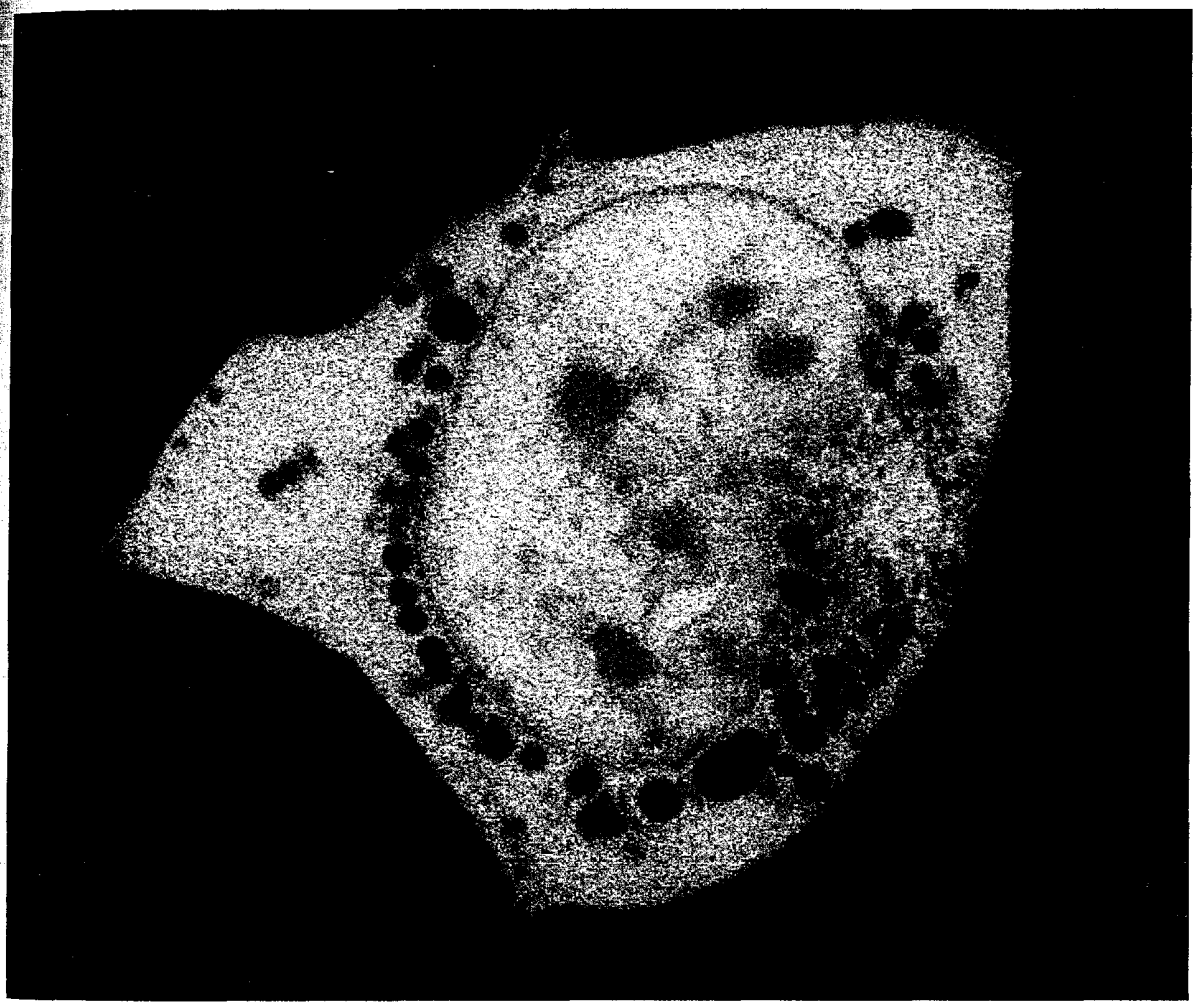

FIGURE 78.1
Confocal microscopy image of GFP labeling. Confocal microscopy imaging shows the distribution of labeling by GFP throughout the cell. (Photo provided by B. Chazotte, University of North Carolina.)

(Moriyoshi et al. 1996), nucleus (Davis et al. 1995), Golgi complex (Cole et al. 1996), peroxisome (Kalish et al. 1996), and mitochondria (Rizzuto et al. 1995). Targeting GFP to a small compartment, thereby concentrating the protein, can be an efficient way of making it easier to detect the protein even at low levels of expression (Haseloff et al. 1997).

More than just a targeting sequence can be attached to GFP. By creating fusion constructs in which the entire coding region of a particular protein and GFP are fused, it has been possible to follow functional, full-length proteins as they are used by living cells. The relatively large size of GFP makes it difficult to envision how its addition would not perturb the function of the target protein, but there is a growing body of evidence that the addition of GFP can be benign and that this strategy can produce important insights. GFP has been fused, without an apparent disruption of function, to a variety of proteins including a transcription factor (Wang and Hazelrigg 1994), a histone (Salmon et al. 1994), a pre-mRNA splicing factor (Misteli et al. 1997), a nuclear receptor involved in olfaction (Sengupta et al. 1994), a subunit of the translation-release factor responsible for the termination of translation (Patino et al. 1996), microtubule-associated proteins (Kahana et al. 1995; Olson et al. 1995), a protein involved in sister-chromatid cohesion (Nabeshima et al. 1995), and a glutamate-gated ion channel (Marshall et al. 1995).

GFP and the Fourth Dimension

Perhaps the greatest strength of GFP as a tool is that it can be followed in living cells, making it possible to study dynamic systems in ways that were previously not feasible. Experiments can move beyond the typical two- or three-dimensional data sets of spatial localization into the realm of time. The simplest way of doing so is time-lapse photography or computer acquisition of images. This has already provided new and intriguing views of cell and protein movement and offers tremendous opportunities (for details of live cell microscopy, see Chapters 75–76). The movement of defined cells during embryogenesis (Peters et al. 1995) or the maturation of a neuron's processes can be followed in real time (Chalfie et al. 1994; Moriyoshi et al. 1996). GFP fusion constructs have been used to study the spindle pole body in yeast (Kahana et al. 1995; Nabeshima et al. 1995), the kinetics of actin (Doyle and Botstein 1996) or myosin (Moores et al. 1996), the centromere during meiosis (Kerrebrock et al. 1995), and coronin during phagocytosis (Maniak et al. 1995).

There are two simple ways of probing the mobility of a GFP tagged protein. First, photobleaching can be used to study fluorescent recovery in particular parts or compartments of a cell (Cole et al. 1996; for details of photobleaching, see Chapter 79). Second, GFP can be used in experiments that are essentially the inverse of a photobleaching paradigm. In the wild-type protein, UV light causes a photoisomerization such that the blue absorption of the protein increases (Cubitt et al. 1995). This property enabled Yokoe and Meyer (1996) to photoisomerize (with a laser emitting at 365 nm) small pools of a K-ras-GFP fusion protein within a cell and then image (using the 488-nm line of a confocal microscope) the local increase in fluorescence.

In the future, it may be possible to use GFP to probe protein interactions in living cells. Different mutants of GFP, which differ in their excitation/emission properties, could be used as tags on two different proteins. Fluorescence resonance energy transfer between the two forms of GFP would then provide a means to measure

the interaction of these proteins. It has been demonstrated that this powerful approach is technically feasible in solution (Heim and Tsien 1996; Mitra et al. 1996), but much remains to be determined concerning the utility of this strategy in living cells.

THE SEQUENCES

Many different clones encoding GFP are now available. Listed below are some of the most useful ones that have been deposited in GenBank.

GenBank Accession#: M62654 is the original clone isolated by Prasher et al. (1992). It has been widely distributed and was the basis for most of the original GFP constructs. This clone was accidentally mutated during PCR amplification (Q80R) to construct pGFP 10.1 (Chalfie et al. 1994); this appears to have no effect on the function of the protein. However, the Q80R mutation has been incorporated into many of the constructs now in use.

GenBank Accession#: U73901 is the GFPmut3 sequence (Cormack et al. 1996) that was significantly brighter than gpf10 when expressed in *E. coli.* It contains the mutations S65G, S72A in the original jellyfish codon usage background.

GenBank Accession#: U50963 was modified (Zolotkin et al. 1996) such that the Kozak site and 85 codons were changed to optimize expression in mammalian cells, and the S65T mutation was introduced to increase excitation in the blue. This is commercially available (Life Technologies) in a cytomegalovirus (CMV) expression vector (pGreenLantern).

GenBank Accession#: X96418 is a clone in which the codon usage was optimized for expression in plants (G.J.A. Rouwendal et al., unpubl.).

GenBank Accession#: U19276 (phGFP-S65T) is a commercially available (Clontech) CMV expression construct with the S65T mutant form of GFP in a humanized codon usage background. This construct is analogous to GenBank Accession#: U50963, but the sequences (codons chosen) are quite different.

GenBank Accession#: U87624 is a clone in which the codons were altered to remove the cryptic splice site that impairs expression in plants (Haseloff and Amos 1995).

GenBank Accession#: U17997 is a commercially available (Clontech) form of the original GFP used by Chalifie et al. (1994; known as TU#60, containing the Q80R mutation).

GenBank Accession#: U55763 is one of three analogous vectors designed to create fusion constructs that place GFP at the amino terminus of the target protein (commercially available from Clontech). The GFP-coding sequence contains the F64L, S65T mutations (known as GFPmutl; Cormack et al. 1996) and an H231L mutation in a human codon usage background. This is not the same codon usage optimization as that used by Zolotkin and colleagues (1996) to produce GenBank Accession#: U50963.

GenBank Accession#: U55762 is one of three analogous vectors designed to create fusion constructs that place GFP at the carboxyl terminus of the target protein (commercially available from Clontech). The GFP-coding sequence contains the

F64L, S65T mutations (known as GFPmut1; Cormack et al. 1996) and an H231L mutation in a human codon usage background. This is not the same codon usage optimization as that used by Zolotkin and colleagues (1996) to produce GenBank Accession#: U50963.

Clones, fusion constructs, and constructs for expression of GFP in mammalian cells are commercially available from many suppliers including, Invitrogen, Quantum Biotechnologies, Life Technologies, and Clontech Laboratories.

INTERNET RESOURCES

A bionet mail list of recent questions concerning GFP can be found at

http://www.bio.net/hypermail/FLUORESCENT-PROTEINS/

The most recent information about the GFP vectors created by Clontech can be found at

http://www.clontech.com/clontech/Catalog/GeneExpression/GFPintro.html

Information about the GFP vectors and mutants sold by Quantum biotechnologies Inc. can be found at

http://www.qbi.com/autofluo.html

The latest on GFP expression vectors created by Invitrogen can be found at

http://www.invitrogen.com/

Technical information about pGreenLantern can be found at Life Technologies.

http://www.lifetech.com/cgi-bin/pages.pl?page=online

The features of the vector and the sequence of the construct can be found there.

The structure of GFP can be found at Brookhaven National Laboratory.

http://www.pdb.bnl.gov/browse __ it.html

The stucture of wild-type GFP (Yang et al. 1996) is I.D. code 1gfl, and the structure of the S65T mutant (Ormö et al. 1996) is I.D. code 1 ema.

To view the most recent movies of GFP-tagged proteins, see the CSHL web site for pointers.

How to attach fluorophores:

- chemical bond
- antibodies, peptides, aptamers etc.
- GFP-constructs
- intrinsic fluorescence

Cell-substrate adhesions, however, can be contrasted in white light as well. A standard 50% T/R plane glass reflector is used to illuminate the specimen as shown in Figure 94.3. To improve the signal-to-noise ratio at the low reflectivities of cell and substrate (<4%), the field diaphragm may be set to less than the full field diameter. The field diaphragm further serves as a focusing aid as it comes into sharp focus only when the cover glass is in focus. Special so-called antiflex objectives further enhance signal-to-noise ratios by eliminating all residual internal scatter in the objective using a crossed polarizer and analyzer in the microscope while a $\lambda/4$ plate in front of the objective in effect rotates the signal waves from the specimen $2 \times 45°$ for free passage through the analyzer. Furthermore, RIM can be greatly enhanced by using video image processing (see Chapter 95).

FLUORESCENCE MICROSCOPY

A wide range of specimens absorb light radiation, become "excited," and then re-radiate or emit light. When the emission continues for some time after excitation, the process is called phosphorescence. Emission that ceases almost instantly after excitation ($\sim 10^{-7}$ seconds) is called fluorescence. Both forms of emitted radiation, along with chemical reactions that cause light emission, all comprise photoluminescence, an area of growing interest to the experimental biologist.

Many organic and some inorganic substances (e.g., drugs, vitamins, and chlorophyll) display autofluorescence or primary fluorescence: When irradiated with light of a specific spectral region, they emit radiation of longer wavelength (lower energy). Stokes observed this in fluorspar, and the spectral relationship he described between excitation and emission became Stokes' law. The study of primary fluorescence dates back to the early part of this century with the investigations of Köhler, Reichert, and others. Fluorescence microscopy garnered serious attention only in the 1950s, after Coons and Kaplan successfully developed indirect immunofluorescence for specific staining of tissues and cells with fluorescent compounds (e.g., FITC) conjugated to an antibody, thereby detecting and localizing specific antigens within cells.

Labeling tissues and cellular components with proteins (e.g., antibodies) and nucleic acids derivatized directly or indirectly with specific fluorochromes has become one of the most important methods for both research and clinical diagnostic studies. The range of fluorescence markers or labels for every conceivable cellular organelle, protein, and nucleic acid component is steadily growing. For example, techniques ranging from cellular pH or dynamic events involving Ca^{++} fluxes in vivo (see Chapter 80) to fluorescence in situ hybridization (FISH; see Chaper 111) for localizing specific genes in situ have revolutionized many aspects of cell biology and diagnostic pathology. It should be noted that both confocal microscopy (see Chapter 96) and two-photon or multiphoton microscopy (see Chapter 97) also employ fluorescence. The following factors make fluorescence such an important tool in cell and molecular biology.

- *Specificity:* Fluorescent molecules or fluorochromes have specific absorption and emission wavelengths.
- *Sensitivity:* Under optimum conditions, a single fluorochrome can be detected.
- *Spectral sensitivity:* Excitation and/or emission wavelengths of certain fluorochromes can reflect physiological, physical, and/or chemical changes (e.g., ratio imaging).

Obtaining High-quality Fluorescence Images

In addition to the appropriate light source and the proper optics, selection of the best filters is essential. The exciting radiation is intense and covers the whole field, and only small portions of the field emit relatively weak fluorescence signals. The exciting, shorter-wavelength light must be blocked, after traversing the specimen, permitting only the longer-wavelength fluorescence to pass to the eye or detector. This is accomplished with two filters whose transmission curves optimize the excitation and emission wavelengths, for a given fluorochrome, without overlapping areas of transmission. The primary, or excitation, filter is used to select wavelengths from the light source corresponding to those in the excitation spectrum of the fluorochrome and to reflect or absorb other wavelengths (Fig. 94.25A). This primary filter is placed in the illumination beam. The secondary, or barrier, filter separates unabsorbed excitation light from fluorescence emission light (most excitation light is in fact not absorbed by the fluorochrome) and is placed in the observation path (see Fig. 94.25B).

Transmitted Fluorescence versus Epifluorescence Microscopy

Fluorescence was initially studied with the transmitted light microscope. For best a priori separation of emitted from exciting radiation, usually a dark-field condenser is used (see discussion of dark-field microscopy above). Presently, transmitted light fluorescence is limited to low-magnification objectives ($<10\times$), where the relatively higher condenser aperture provides more intense excitation energy and offsets the generally lower-objective aperture with its limited light gathering power.

The most widely used contemporary fluorescence microscopes are equipped with incident or epiillumination and incorporate the use of a dichroic mirror—or chromatic beam splitter—to assist in the separation of the fluorescence emission light from unabsorbed reflected excitation light. The surfaces of dichroic mirrors have thin coatings that facilitate the reflection of shorter wavelengths and transmission of longer wavelengths (see Fig. 94.25).

The advent of highly efficient chromatic beam splitters or dichroic reflectors has made epifluorescence the method of choice for most applications. The advantages are obvious.

- The exciting radiation travels in a path opposite to that of the observed fluorescence. This minimizes the effects of the absorption of light due to specimen thickness.
- The full-objective aperture provides excitation and collects emitted fluorescence for maximum brightness.
- The objective becomes the condenser assuring perfect alignment between both.
- Epifluorescence can be readily combined with other transmitted light techniques such as Phase or DIC. It is often critical to find specimen areas of interest with these latter techniques prior to subjecting the specimen to excitation in order to reduce quenching or fading of fluorescence intensity.
- Only the objective needs to be immersed in oil for studies using the highest NA.

Figure 94.26 shows typical transmission curves for some of the exciter and barrier filters. Broad band (dyed glass filters), band pass (BP), short pass (KP), and long pass (LP) interference filters are designed and combined to provide the highest possible transmission for the excitation (absorption) wavelength range of a given

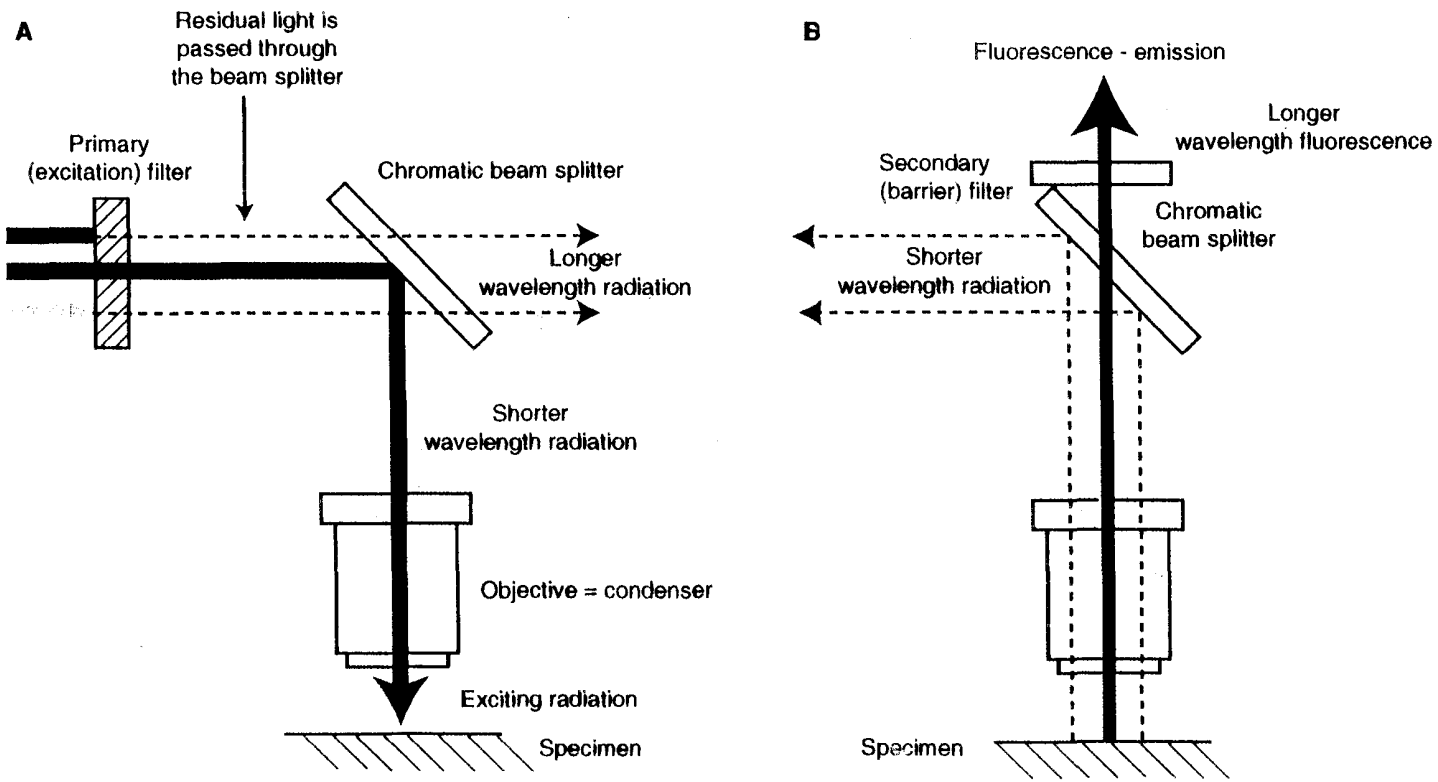

FIGURE 94.25
Filter components of the epifluorescence microscope. The blue excitation light and the green light emitted from the specimen are typical for the fluorochrome fluorescein.

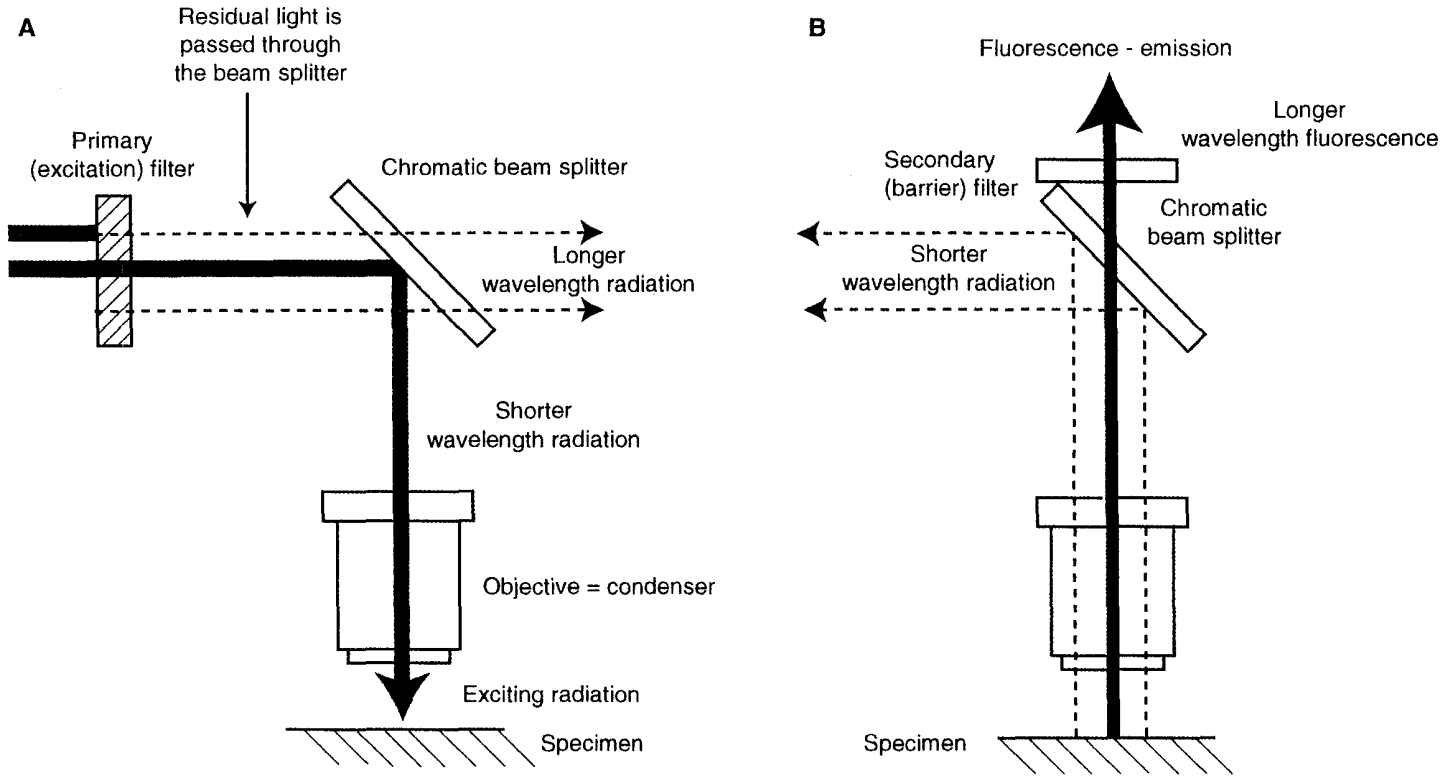

FIGURE 94.25
Filter components of the epifluorescence microscope. The blue excitation light and the green light emitted from the specimen are typical for the fluorochrome fluorescein.

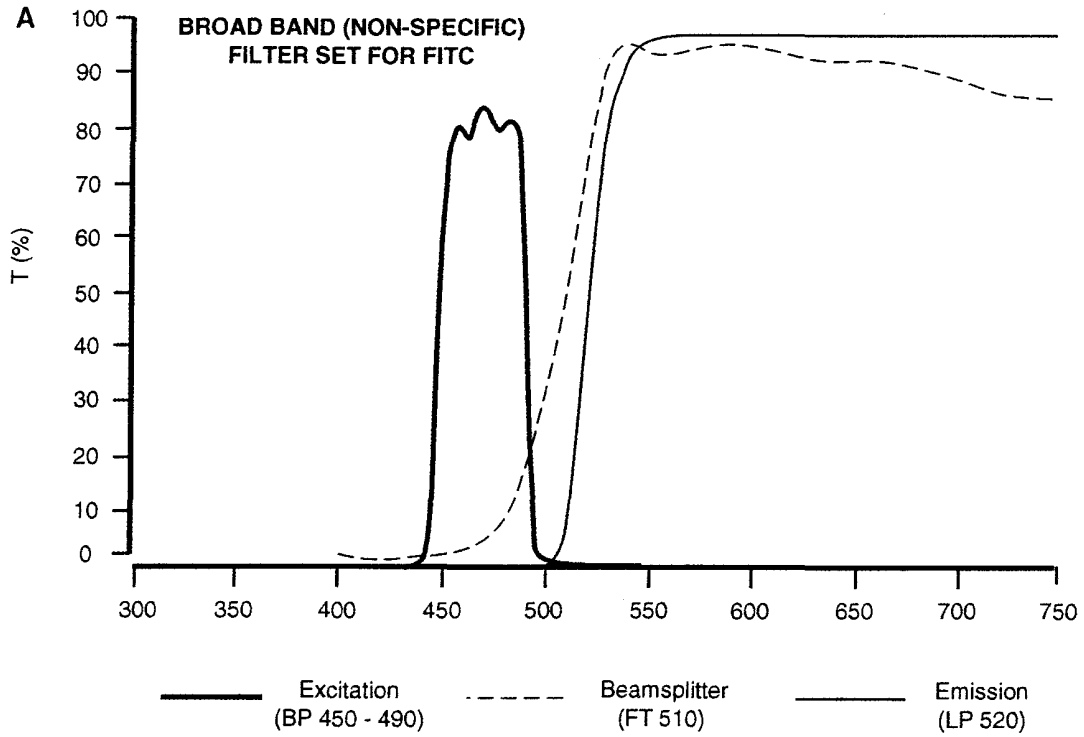
A
BROAD BAND (NON-SPECIFIC)
FILTER SET FOR FITC
T (%)
100
90
80
70
60
50
40
30
20
10
0
300
350
400
450
500
550
600
650
700
750
Excitation
(BP 450 - 490)
Beamsplitter
(FT 510)
Emission
(LP 520)

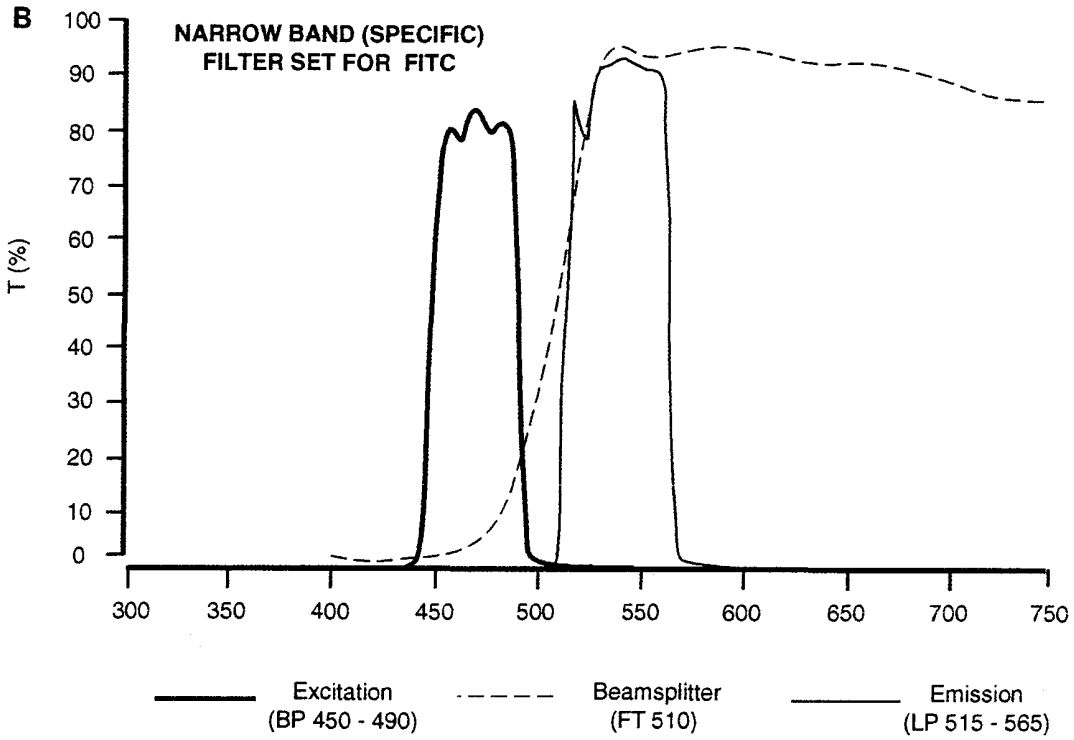
B
NARROW BAND (SPECIFIC)
FILTER SET FOR FITC
T (%)
100
90
80
70
60
50
40
30
20
10
0
300
350
400
450
500
550
600
650
700
750
Excitation
(BP 450 - 490)
Beamsplitter
(FT 510)
Emission
(LP 515 - 565)

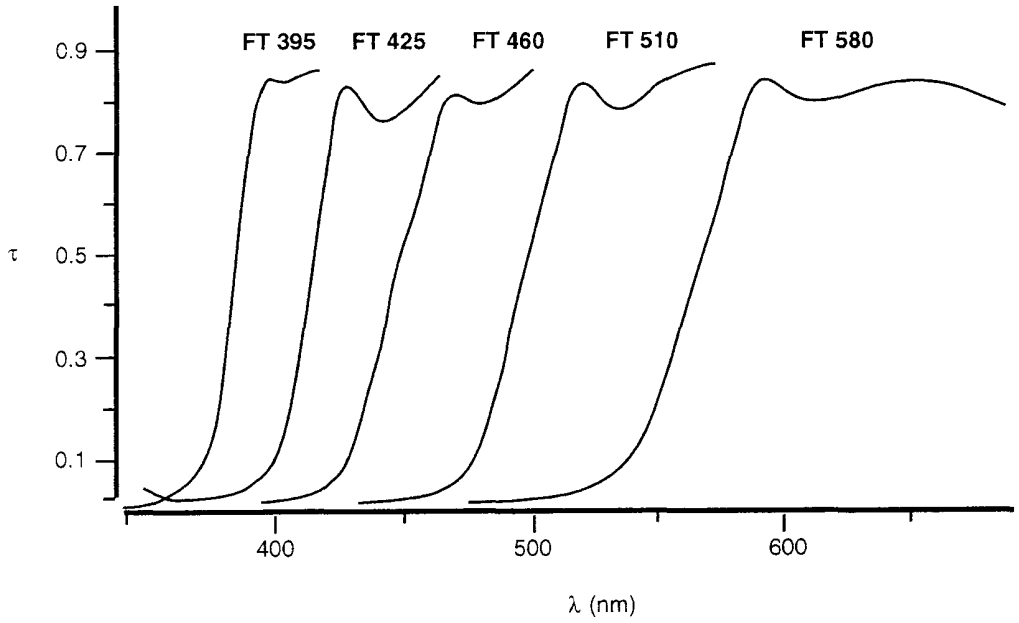

FIGURE 94.27
Transmission of typical chromatic beam splitters. "Tau" (τ) represents transmission.

fluorochrome (exciter filter) and the highest transmission for the fluorochrome's emitted fluorescence light (barrier filter). A minimum of overlap of the transmission curves of exciter and barrier filters (crosstalk) assure the best contrast (S/N) in the image. The spectral characteristics of a typical chromatic beam splitter are shown in Figure 94.27. Filter combinations are available for a wide range of fluorochromes useful in cell biological studies (see Appendix 3).

Exciter filters, chromatic beam splitters, and barrier filters are usually mounted in either sliders, filter blocks, or external filter wheels for quick insertion into the light path for a range of different fluorochromes.

> *Caution:* Chromatic beam splitters have exposed thin layers of soft interference coatings that should not be touched or wiped!

Light Sources for Fluorescence

Choosing the best light source is primarily dictated by the absorption (excitation) peak of the fluorochrome to be used (see Appendix 3). In addition, however, many filter sets contain exciter filters specifically designed for the intense emission lines of mercury arc lamps at wavelengths of 365, 405, 436, and 546 nm and therefore mandate the use of a mercury burner (see below). Other considerations are based on the fact that some fluorophores have absorption peaks in spectral regions where a xenon lamp has relatively more output (FITC at 480 nm) or where even a tungsten halogen lamp may suffice (e.g., with the use of low-light-level video; see Chapter 95)

FIGURE 94.26
Transmission curves for some typical exciter and barrier filters. (*A*) Broad-band (nonspecific) filter set for FITC. (*B*) Narrow-band (specific) filter set for FITC.

and may actually minimize fading of fluorescence, often encountered with FITC and mercury lamps. For further information, refer to the relative spectral intensity curves under light sources for the microscope covered below.

Optimal Alignment of the Light Source

Aligning the light source optimally in an epifluorescence microscope, particularly a DC-source such as the HBO 100, is critical for a uniformly illuminated field. Follow the manufacturer's instructions carefully to achieve maximal illumination. Below is a typical procedure for mercury/xenon lamp exchange and alignment.

1. Remove the old lamp by following instructions outlined in the illuminator manual.

   Never touch the bulb with your hands! If you do touch the bulb, gently wipe off the fingerprints with 100% ethanol. If this precaution is not taken, the bulb will become etched when turned on due to the intense heat output of these light sources.

   Remember, when placing the arc lamp into the socket, try to line up the heat sink so that it is parallel to the front of the socket. Because the lamp housing is compact, it will be easier to position the socket into the housing with the heat sink lined up!

2. After placing the arc lamp and the socket into the housing, turn on the power, and open any shutters and iris diaphragms in the light path. Use an open position in the nosepiece to allow the light to be projected down to the stage area. Place a white piece of paper on the stage and move the epireflector/filter holder to a position that reduces light intensity to a comfortable level.

   This basic method for lamp alignment is also used for transmitted light optical systems.

3. Adjust the lamp collector focusing control so that the real and mirror images of the lamp are sharply focused. The mirror image is obtained with the reflecting mirror mounted behind the lamp. Adjust the up and down control of the real image (move the socket up and down) until both the real and mirror images are visible on the paper.

4. Adjust the focus/size of the mirror image using the mirror position control screws so that the focus and size of the mirror image match that of the real image.

5. Fine-tune the adjustment screws so that the real image is located close to center.

6. Once the real image is positioned, move the mirror image using the left and right controls and the up and down controls so that the mirror image is located symmetrical to the real image.

7. After inserting the objective of choice, use the collector lens focus control (Fig. 94.2B) until uniform field illumination is achieved. Different objectives require slightly different adjustments to the collector focus control for even field illumination.

   Figure 94.28 illustrates proper alignment of the light source in epifluorescence microscopy. Allow a newly installed bulb to burn for at least 2 hours before turning it off. Always remember

The picture of a

telephone

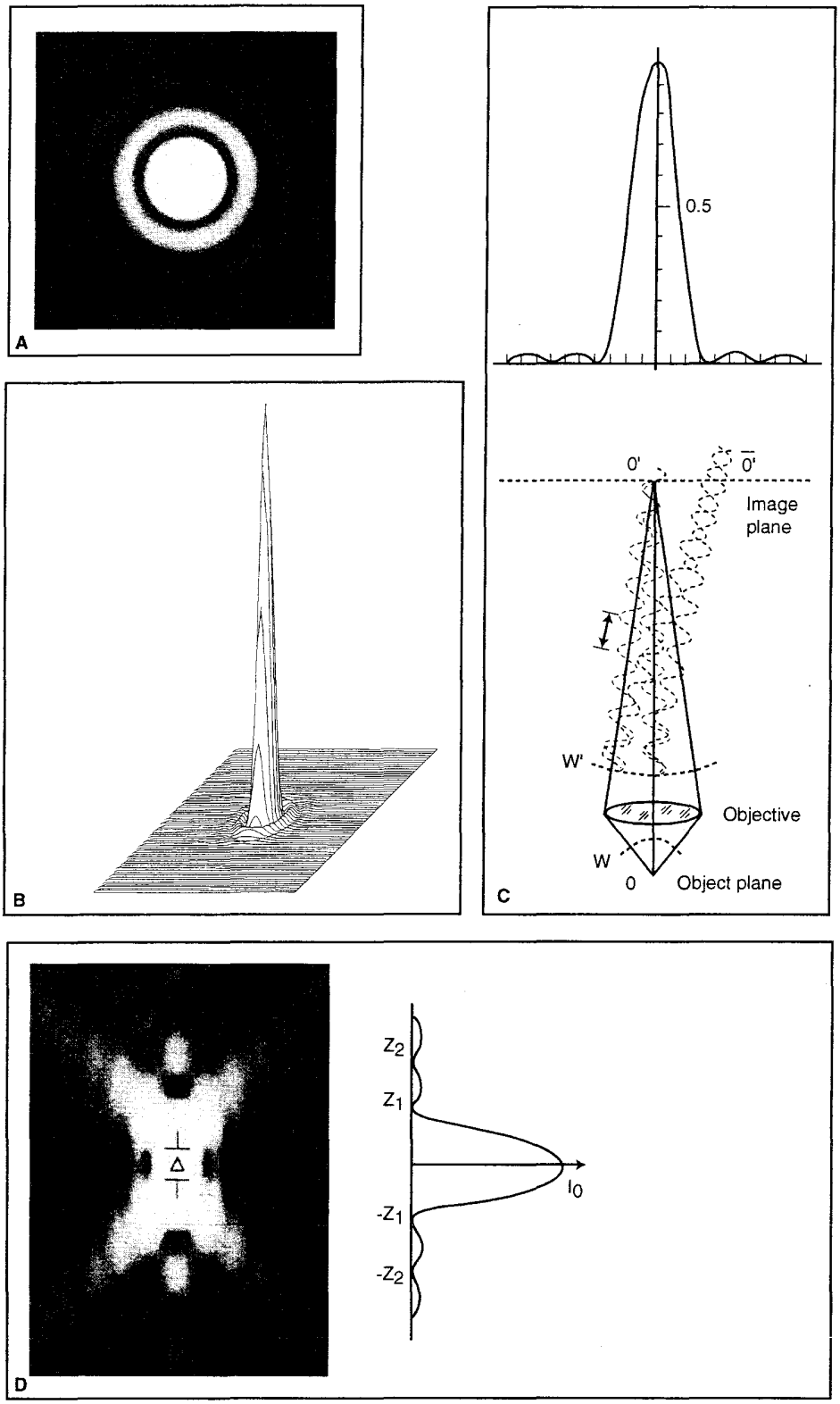
A
0.5
B
0'
0'
Image
plane
W'
Objective
W
0
Object plane
C
Z2
Z1
-Z1
-Z2
I0
D

The numerical aperture (NA) of the lens is a function of the light-collecting ability of the lens, or a measure of the "cone of light" entering the objective from a fixed object distance. The refractive index (n) of a material represents the optical density (e.g., the speed of propagation of light rays) between materials such as glass and air. Typically, the space between the objective lens and the specimen is air, which has a refractive index of about 1. Special lenses called oil immersion lenses function with oil rather than air in this space. Immersion oil has a refractive index of about 1.5. Therefore, with oil immersion lenses, resolution is increased (see below). Furthermore, because glass and immersion oil have the same refractive index, no light is lost through reflection from the surface of the lens and the cover glass. Therefore, the higher the refractive index, the smaller the resolvable distance between two points and the better the resolution. This can be explained as follows. In Figure 94.4, the dark ring around the central bright disc represents a zone of destructively interfering diffracted wavefronts and defines the diameter of the disc. Using this diameter, Rayleigh set the limit for the smallest resolvable distance between 2 points at

$$d = \frac{1.22 \times \lambda}{2 \times \mathrm{NA}}$$

This resolution limit for self-luminous objects (fluorescence) can be exceeded somewhat by confocal microscopes (see Chapter 96) and by electronic image processing, but it provides a good rule of thumb for visual observation and photomicrography.

The Abbe Limit of Resolution for Illuminated Objects

Diffraction also takes place within the object when it is illuminated in the microscope. Constructive interference between two diffracted wavefronts from adjacent points within the object, separated by a distance "d" (Fig. 94.5A), generates new plane waves (diffraction orders) at the diffraction angle (Fig. 94.5B). The following relationship develops from this phenomenon:

$$\mathrm{NA} = \frac{\lambda}{d} \quad \text{or} \quad d = \frac{\lambda}{\mathrm{NA}}$$

This relationship assumes illumination parallel to the optical axis.

Abbe postulated that for two points to be resolved, at least two adjacent orders of diffracted light (see Fig. 94.5) produced by their spacing d must be collected by the objective. The NA of an objective directly determines its ability to collect diffracted wavefronts that emanate from the object.

Either diffracted and nondiffracted wavefronts or two orders of diffracted light

FIGURE 94.4
Generation of the Airy disc. It is the Airy disc phenomenon that limits resolution in light microscopy. With the highest numerical aperture objective (e.g., 1.4), the Airy disc phenomenon limits resolution to approximately 0.2 μm. (*A*) Micrograph of the Airy disc generated by a 0.2 μm pinhole. This represents a cross-sectional view through the Airy body in the image plane. (*B*) Light intensity distribution across an Airy disc. (*C*) Diagrammatic representation of wavefronts diffracted by the objective aperture and their constructive (0′) and destructive ($\bar{0}'$) interference. This results in the dark and light concentric rings seen in *A*. The light intensity plot across the image plane is seen above the dotted line. (*D*) This diagram represents a section through the Airy body in the optical (Z) axis (perpendicular to the image plane), and its intensity distribution.

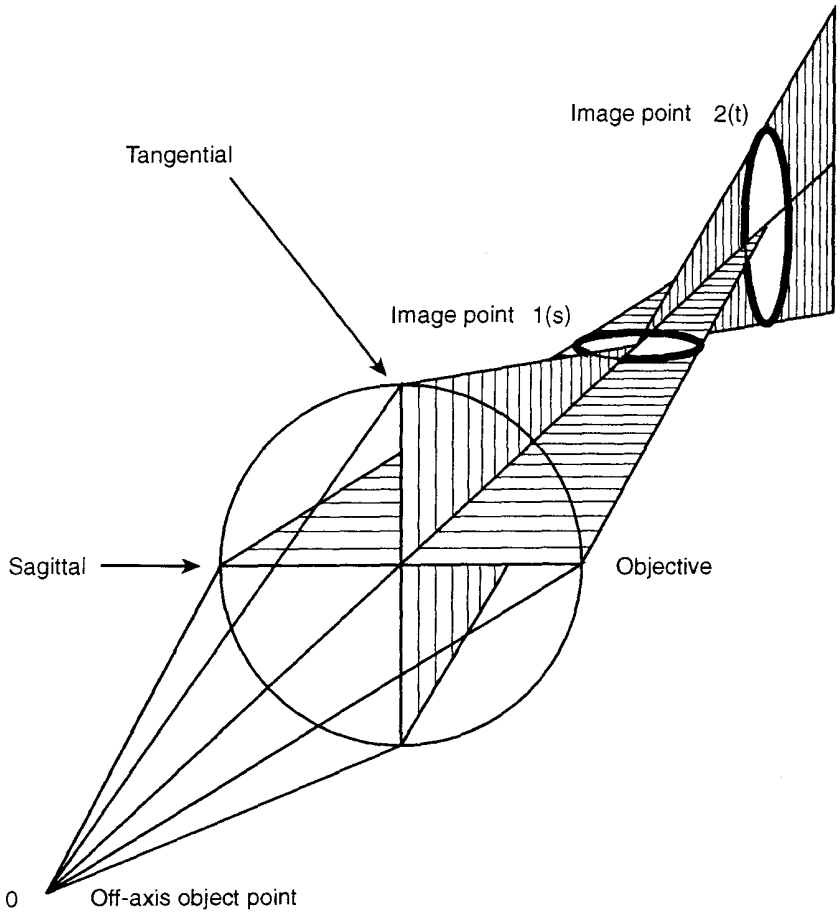

FIGURE 94.13
Astigmatism. Tangential (t) and sagittal (s) cross-sections through the objective form different image locations from the optical axis for off-axis points. Depending on the focus, the point becomes tangentially or radially distorted. Note that the further off axis an object point is, the more distorted its image becomes.

Below is a summary of useful formulas:

Numerical aperture: $\mathrm{NA} = n \sin \alpha$

Resolution: $d = \dfrac{\lambda}{\mathrm{NA\ obj.} + \mathrm{NA\ cond.}}$

Useful magnification: $= 500 - 1000 \times \mathrm{NA}$

Field of view (mm in specimen) $= \dfrac{\text{field of view number * of eyepiece}}{\text{Magn. obj.} \times \text{mag. Ch'ger (e.g., optovar)}}$

Depth of field $\mathrm{T\ (mm)} = \dfrac{1000}{7 \times \mathrm{NA\ obj.} \times \text{mag. total}} + \dfrac{\lambda}{2 \times \mathrm{NA\ Obj.}^2}$

*The diameter of the field-limiting fixed stop in the eyepiece in millimeters is usually marked on the eyepiece after the magnification.

Point spread function

From Wikipedia, the free encyclopedia

The **point spread function** (**PSF**) describes the response of an imaging system to a point source or point object. A related but more general term for the PSF is a system's impulse response. The PSF in many contexts can be thought of as the extended blob in an image that represents an unresolved object. In functional terms it is the spatial domain version of the modulation transfer function. It is a useful concept in Fourier optics, astronomical imaging, electron microscopy and other imaging techniques such as 3D microscopy (like in Confocal laser scanning microscopy) and fluorescence microscopy. The degree of spreading (blurring) of the point object is a measure for the quality of an imaging system. In incoherent imaging systems such as fluorescent microscopes, telescopes or optical microscopes, the image formation process is linear in power and described by linear system theory. When the light has coherence (physics), image formation is linear in complex field. This means that when two objects A and B are imaged simultaneously, the result is equal to the sum of the independently imaged objects. In other words: the imaging of A is unaffected by the imaging of B and *vice versa*, owing to the non-interacting property of photons. (The sum is of the light waves which may result in destructive and constructive interference at non-image planes.)

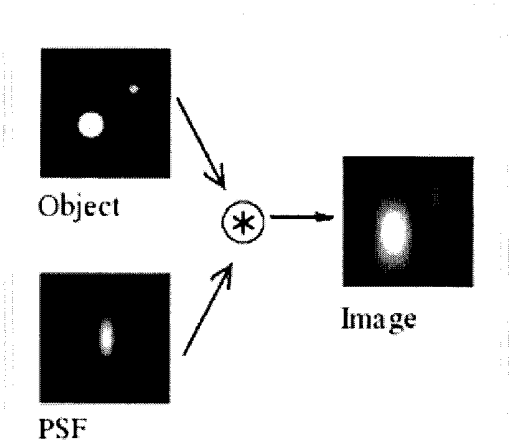

Image formation in a confocal microscope: central longitudinal (XZ) slice. The 3D acquired distribution arises from the convolution of the real light sources with the PSF.

Contents

Introduction

By virtue of the linearity property of optical imaging systems, *i.e.*,

$Image(Object_1 + Object_2) = Image(Object_1) + Image(Object_2)$

the image of an object in a microscope or telescope can be computed by expressing the object-plane field as a weighted sum over 2D impulse functions, and then expressing the image plane field as the weighted sum over the *images* of these impulse functions. This is known as the *superposition principle*, valid for linear systems. The images of the individual object-plane impulse functions are called point spread functions, reflecting the fact that a mathematical *point* of light in the object plane is *spread* out to form a finite area in the image plane (in some branches of mathematics and physics, these might be referred to as Green's functions or impulse response functions).

When the object is divided into discrete point objects of varying intensity, the image is computed as a sum of the PSF of each point. As the PSF is typically determined entirely by the imaging system (that is, microscope or telescope), the entire image can be described by knowing the optical properties of the system. This process is usually formulated by a convolution equation. In microscope image processing and astronomy, knowing the PSF of the measuring device is very important for restoring the (original) image with deconvolution.

Theory

The point spread function may be independent of position in the object plane, in which case it is called *shift invariant*. In

addition, if there is no distortion in the system, the image plane coordinates are linearly related to the object plane coordinates via the magnification M as:

$(x_i, y_i) = (M x_o, M y_o)$.

If the imaging system produces an inverted image, we may simply regard the image plane coordinate axes as being reversed from the object plane axes. With these two assumptions, *i.e.*, that the PSF is shift-invariant *and* that there is no distortion, calculating the image plane convolution integral is a straightforward process.

Mathematically, we may represent the object plane field as:

$$O(x_o, y_o) = \int\int O(u, v)\ \delta(x_o - u, y_o - v)\ du\, dv$$

i.e., as a sum over weighted impulse functions, although this is also really just stating the sifting property of 2D delta functions (discussed further below). Rewriting the object transmittance function in the form above allows us to calculate the image plane field as the superposition of the images of each of the individual impulse functions, *i.e.*, as a superposition over weighted point spread functions in the image plane using the *same* weighting function as in the object plane, *i.e.*, $O(x_o,y_o)$. Mathematically, the image is expressed as:

$$\mathrm{field}(x_i, y_i) = \int\int O(u,v)\,\mathrm{PSF}(x_i - Mu, y_i - Mv)\,du$$

in which $\mathrm{PSF}(x_i - Mu, y_i - Mv)$ is the image of the impulse function $\delta(x_o - u, y_o - v)$.

The 2D impulse function may be regarded as the limit (as side dimension w tends to zero) of the "square post" function, shown in the figure below (click to enlarge).

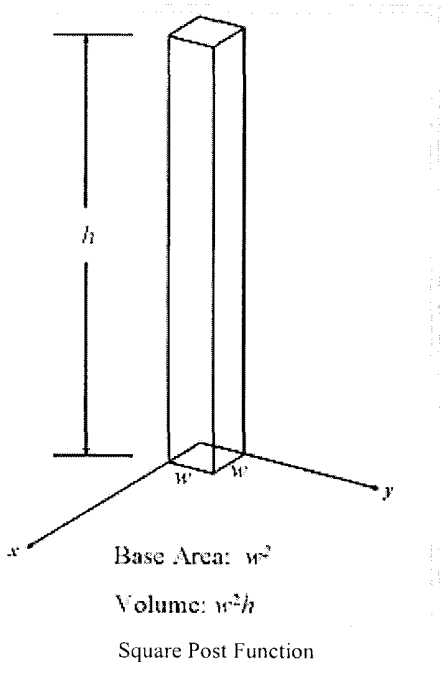

Square Post Function

We imagine the object plane as being decomposed into square areas such as this, with each having its own associated square post function. If the height, h, of the post is maintained at $1/w^2$, then as the side dimension w tends to zero, the height, h, tends to infinity in such a way that the volume (integral) remains constant at 1. This gives the 2D impulse the sifting property (which is implied in the equation above), which says that when the 2D impulse function, $\delta(x - u, y - v)$, is integrated against any other continuous function, $f(u,v)$, it "sifts out" the value of f at the location of the impulse, *i.e.*, at the point (x,y).

Since the concept of a perfect point source object is so central to the idea of PSF, it's worth spending some time on that before proceeding further. First of all, there is no such thing in nature as a perfect mathematical point source radiator; the concept is completely non-physical and is nothing more that a mathematical construct used to model and understand optical imaging systems. The utility of the point source concept comes from the fact that a point source in the 2D object plane can only radiate a perfect uniform-amplitude, spherical wave - a wave having perfectly spherical, outward travelling phase fronts with uniform intensity everywhere on the spheres (see Huygens-Fresnel principle). Such a source of uniform spherical waves is shown in the figure below (click to enlarge). We also note that a perfect point source radiator will not only radiate a uniform spectrum of plane waves, but a uniform spectrum of exponentially decaying (evanescent) waves as well, and it is these which are responsible for resolution finer than one wavelength (see Fourier optics). This follows from the following Fourier transform expression for a 2D impulse function,

$$\delta(x, y) \propto \int\int e^{i(k_x x + k_y y)}\, dk_x\, dk_y$$

The quadratic lens intercepts a *portion* of this spherical wave (and the key phrase here is *a portion*), and refocuses it onto a blurred point in the image plane. For a single lens, an on-axis point

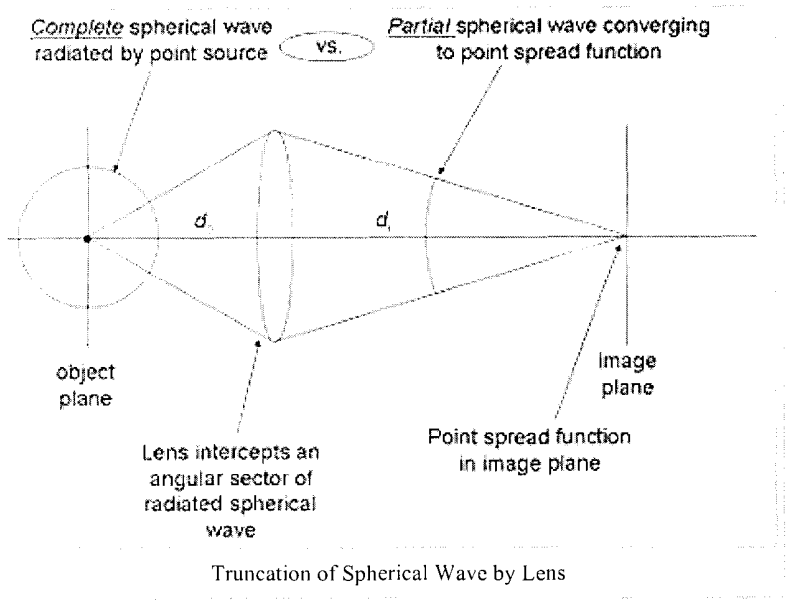

Truncation of Spherical Wave by Lens

source in the object plane produces an Airy disc PSF in the image plane. This comes about in the following way. *It can be shown* (see Fourier optics, Huygens-Fresnel principle, Fraunhofer diffraction) that the field radiated by a planar object (or, by reciprocity, the field converging onto a planar image) is related to its corresponding source (or image) plane distribution via a Fourier transform (FT) relation. In addition, a uniform function over a circular area (in one FT domain) corresponds to the Airy function, $J_1(x)/x$ in the other FT domain, where $J_1(x)$ is the first-order Bessel function of the first kind. That is, a uniformly-illuminated circular aperture radiates an Airy function pattern plus a converging uniform spherical wave (over a circular angular sector) and yields an Airy function image. A graph of a sample 2D Airy function is shown in the adjoining figure (click to enlarge).

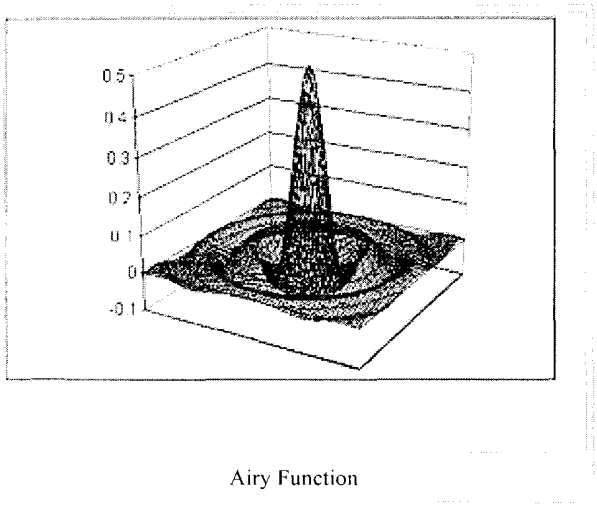

Airy Function

Therefore, the converging (*partial*) spherical wave shown in the figure above produces an Airy disc in the image plane. The argument of the Airy function is important, because this determines the *scaling* of the Airy disc (in other words, how big the disc is in the image plane). If Θ_{max} is the maximum angle that the converging waves make with the lens axis, r is radial distance in the image plane, and wavenumber $k = 2\pi/\lambda$ where λ = wavelength, then the argument of the Airy function is: $kr \sin(\Theta_{max})$. If Θ_{max} is small (only a small portion of the converging spherical wave is available to form the image), then radial distance, r, has to be very large before the total argument of the Airy function moves away from the central spot. In other words, if Θ_{max} is small, the Airy disc is large (which is just another statement of Heisenberg's uncertainty principle for FT pairs, namely that small extent in one domain corresponds to wide extent in the other domain, and the two are related via the *space-bandwidth product*. By virtue of this, high magnification systems, which typically have small values of Θ_{max} (by the Abbe sine condition), can have more blur in the image, owing to the broader PSF. The size of the PSF is proportional to the magnification, so that the blur is no worse in a relative sense, but it is definitely worse in an absolute sense.

History and methods

The diffraction theory of point-spread functions was first studied by Airy in the nineteenth century. He developed an expression for the point-spread function amplitude and intensity of a perfect instrument, free of aberrations (the so-called Airy disc). The theory of aberrated point-spread functions close to the optimum focal plane was studied by the Dutch physicists Fritz Zernike and Nijboer in the 1930–40s. A central role in their analysis is played by Zernike's circle polynomials that allow an efficient representation of the aberrations of any optical system with rotational symmetry. Recent analytic results have made it possible to extend Nijboer and Zernike's approach for point-spread function evaluation to a large volume around the optimum focal point. This Extended Nijboer-Zernike (ENZ) theory (http://www.nijboerzernike.nl/) is instrumental in studying the imperfect imaging of three-dimensional objects in confocal microscopy or astronomy under non-ideal imaging conditions. The ENZ-theory has also been applied to the characterization of optical instruments with respect to their aberration by measuring the through-focus intensity distribution and solving an appropriate inverse problem.

PSF in microscopy

In microscopy, experimental determination of a PSF is usually tricky, due to the difficulty of finding sub-resolution (point-like) radiating sources. Quantum dots and fluorescent beads are usually considered for this purpose.

The PSF in astronomy

In observational astronomy the experimental determination of a PSF is often very straightforward due to the ample supply of point sources (stars or quasars). The form and source of the PSF may vary widely depending on the instrument and the context in which it is used.

For radio telescopes and diffraction-limited space telescopes the dominant terms in the PSF may be inferred from the configuration of the aperture in the Fourier domain. In practice there may be multiple terms contributed by the various components in a complex optical system. A complete description of the PSF will also include diffusion of light (or photo-electrons) in the detector, as well as tracking errors in the spacecraft.

For ground based optical telescopes, atmospheric turbulence (known as astronomical seeing) dominates the contribution to the PSF. In high-resolution ground-based imaging, the PSF is often found to vary with position in the image (an effect called anisoplanatism). In ground based adaptive optics systems the PSF is a combination of the aperture of the system with residual uncorrected atmospheric terms.

Point spread functions in ophthalmology

PSFs have recently become a useful diagnostic tool in clinical ophthalmology. Patients are measured with a wavefront sensor, and special software calculates the PSF for that patient's eye. In this manner a physician can "see" what the patient sees. This method also allows a physician to simulate potential treatments on a patient, and see how those treatments would alter the patient's PSF.

See also

For the closely related topic in general photography, see Circle of confusion.

External links

- PSF calculator (http://support.svi.nl/wiki/NyquistCalculator) for fluorescence microscopes.
- Extended Nijboer-Zernike (ENZ) theory (http://www.nijboerzernike.nl/), calculating the PSF for a general Optical system.

Retrieved from "http://en.wikipedia.org/wiki/Point_spread_function"

Categories: Optics | Ophthalmology

- This page was last modified 00:02, 25 October 2007.
- All text is available under the terms of the GNU Free Documentation License. (See **Copyrights** for details.)
Wikipedia® is a registered trademark of the Wikimedia Foundation, Inc., a U.S. registered 501(c)(3) tax-deductible nonprofit charity.

⇒ Single Particle / Molecule Tracking

fluorophore or gold
≈ 200 – 5 nm pinhole

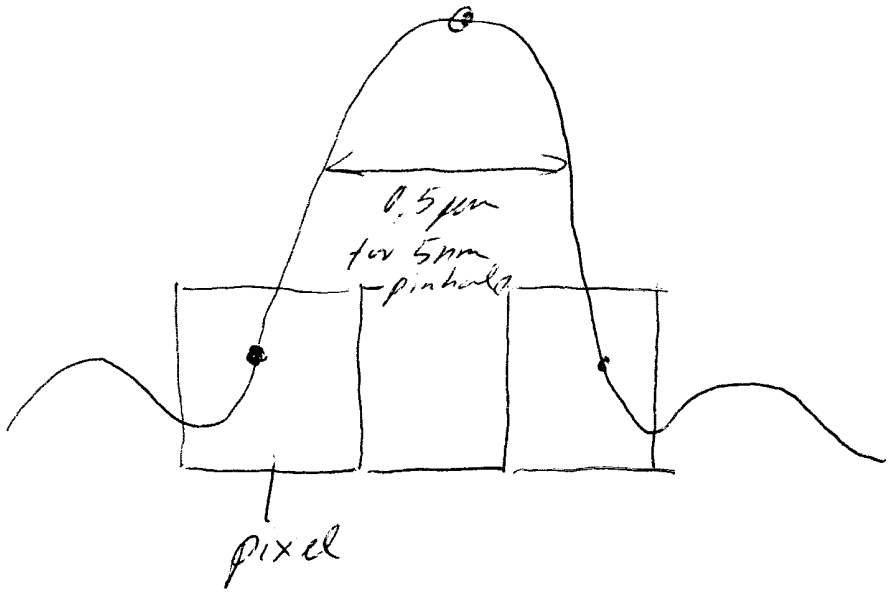

fitting of Airy function through pixel intensity values allows to track the position of an object with a precision of up to ~~Ø~~ 5 nm if the motion is slow enough that the picture is not smeared out and ~~data~~ signal to noise ratio is good enough